

Meteorology of Tropical West Africa: The Forecasters' Handbook

Chapter 6: Nowcasting – Authors: Rita D. Roberts and James W. Wilson

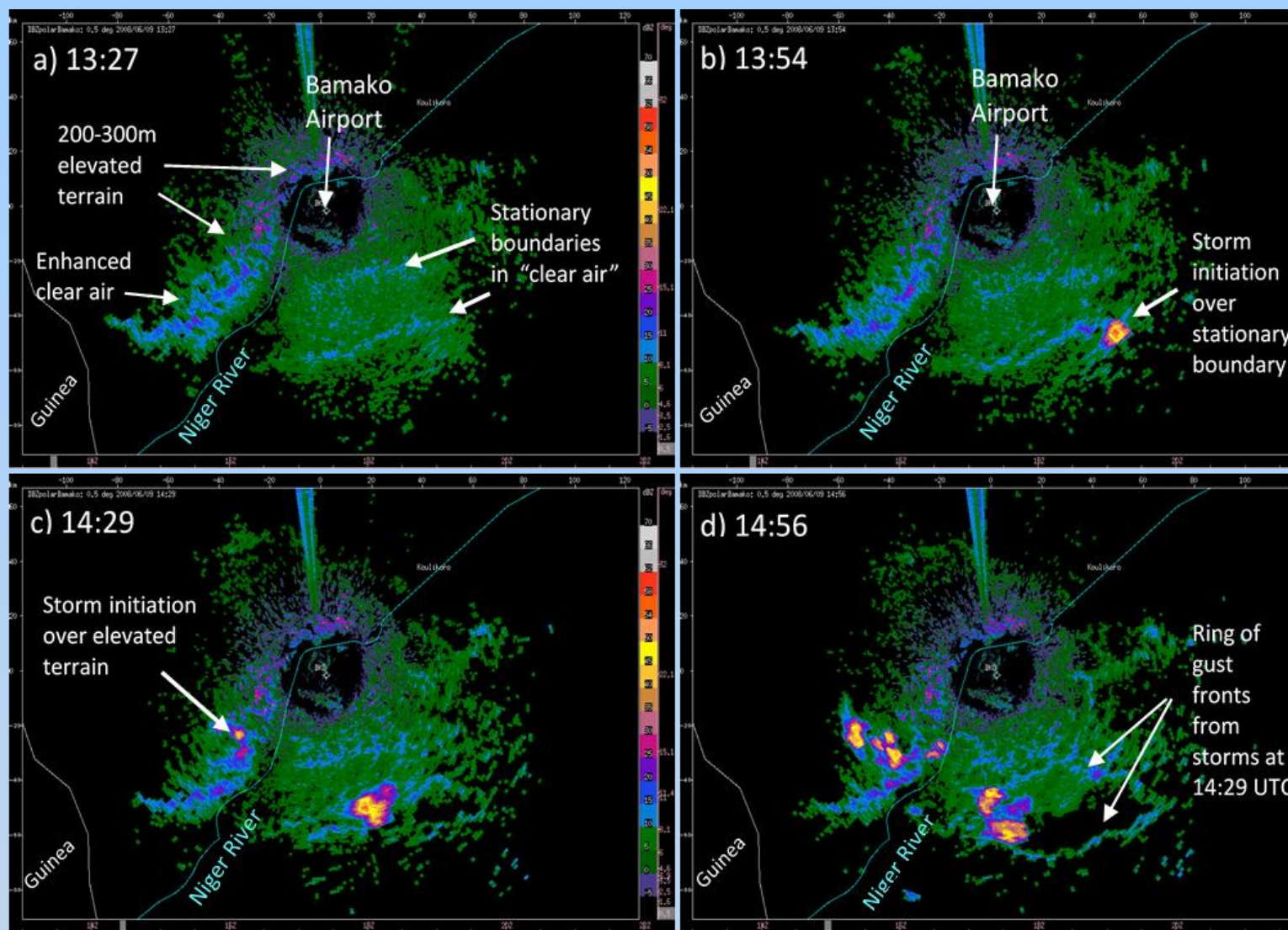


Figure 6.30. Sequence of radar reflectivity images from the Doppler radar located near the Bamako, Mali airport on 9 June 2008 at the four time periods (in UTC) shown. The colour scale is in 5 dBZ increments, with most intense thunderstorms having reflectivities of 50-60 dBZ (orange/red colors). The green and light blue colors in the images represent regions of clear air (no storms). The radar is able to detect clear air because of the backscattering of radio electromagnetic energy from insects in the clear air. (Source: R. Roberts, 2014)

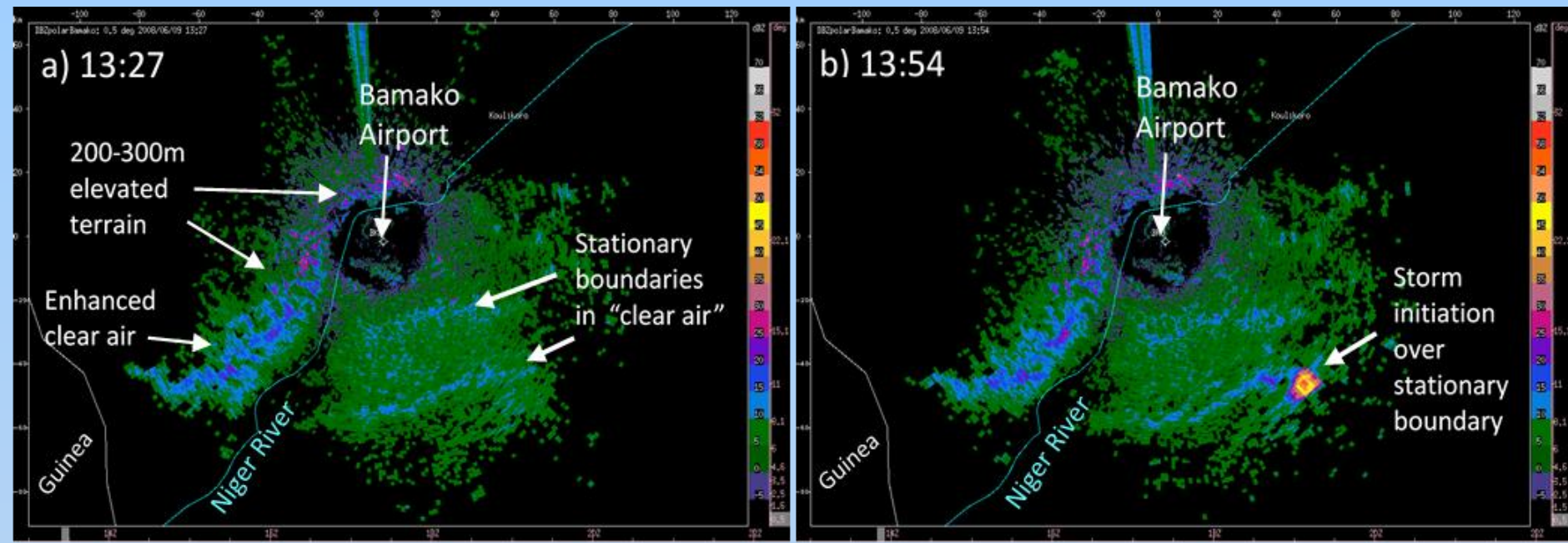


Figure 6.30. Sequence of radar reflectivity images from the Doppler radar located near the Bamako, Mali airport on 9 June 2008 at the four time periods (in UTC) shown. The colour scale is in 5 dBZ increments, with most intense thunderstorms having reflectivities of 50-60 dBZ (orange/red colors). The green and light blue colors in the images represent regions of clear air (no storms). The radar is able to detect clear air because of the backscattering of radio electromagnetic energy from insects in the clear air. (Source: R. Roberts, 2014)

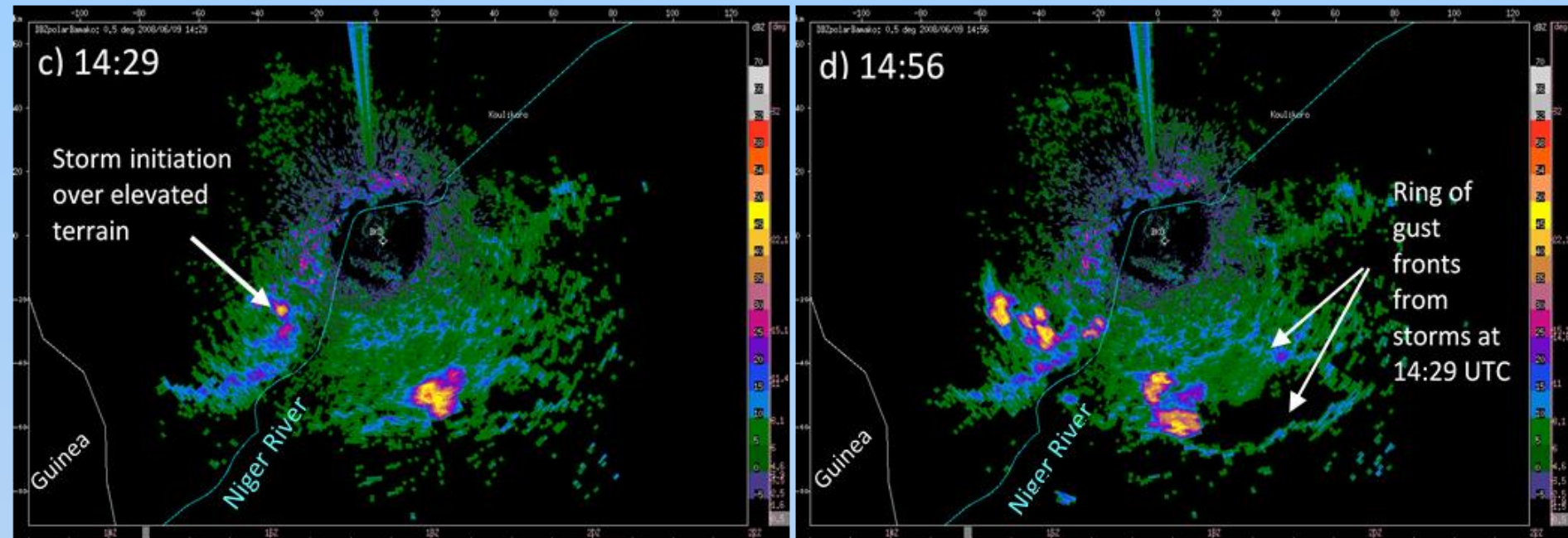
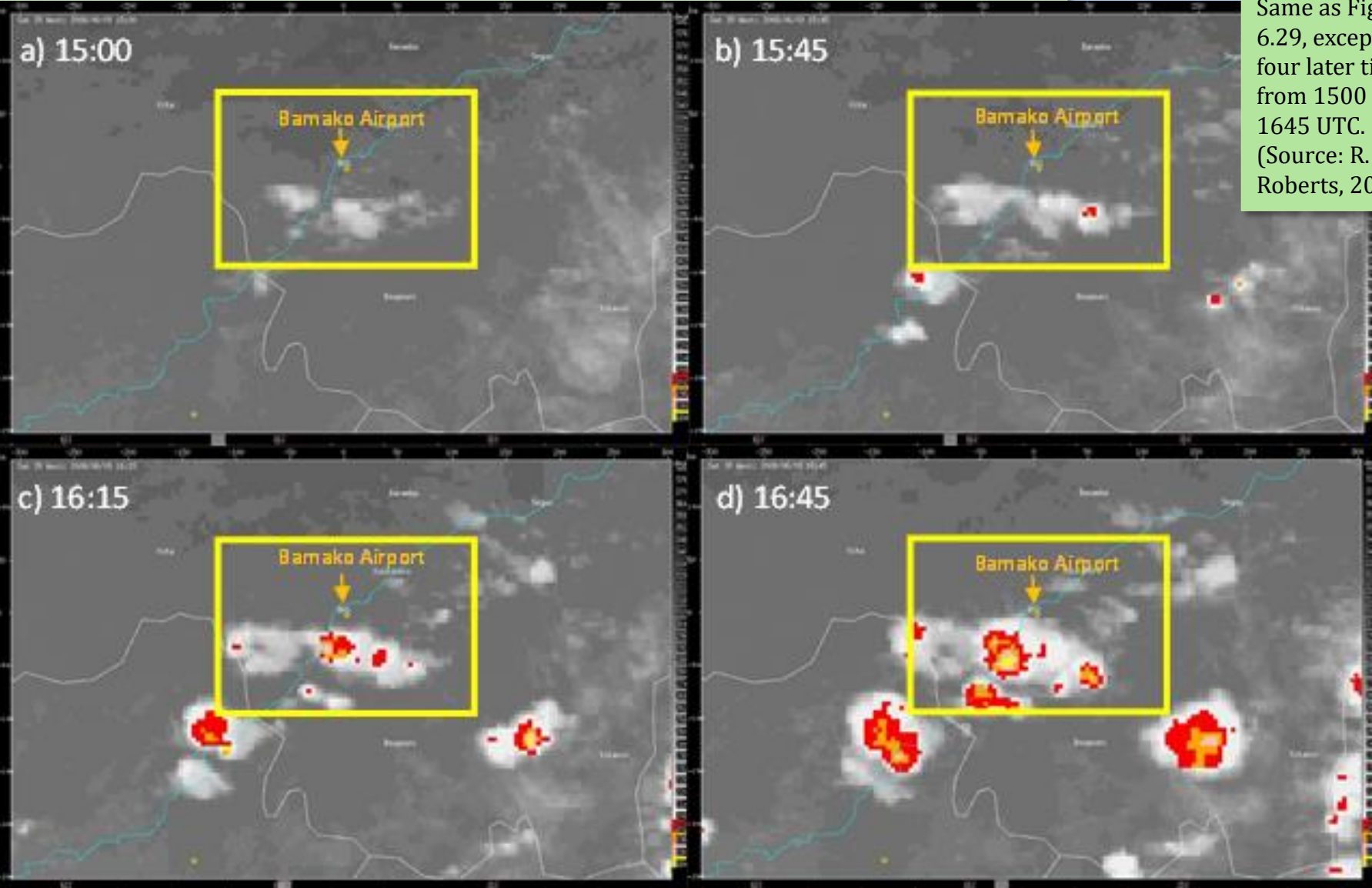


Figure 6.30. Sequence of radar reflectivity images from the Doppler radar located near the Bamako, Mali airport on 9 June 2008 at the four time periods (in UTC) shown. The colour scale is in 5 dBZ increments, with most intense thunderstorms having reflectivities of 50-60 dBZ (orange/red colors). The green and light blue colors in the images represent regions of clear air (no storms). The radar is able to detect clear air because of the backscattering of radio electromagnetic energy from insects in the clear air. (Source: R. Roberts, 2014)

Meteorology of Tropical West Africa: The Forecasters' Handbook

Chapter 6: Nowcasting – Authors: Rita D. Roberts and James W. Wilson

Figure 6.31. Same as Figure 6.29, except at four later time from 1500 - 1645 UTC. (Source: R. Roberts, 2014)



Meteorology of Tropical West Africa: The Forecasters' Handbook

Chapter 6: Nowcasting – Authors: Rita D. Roberts and James W. Wilson

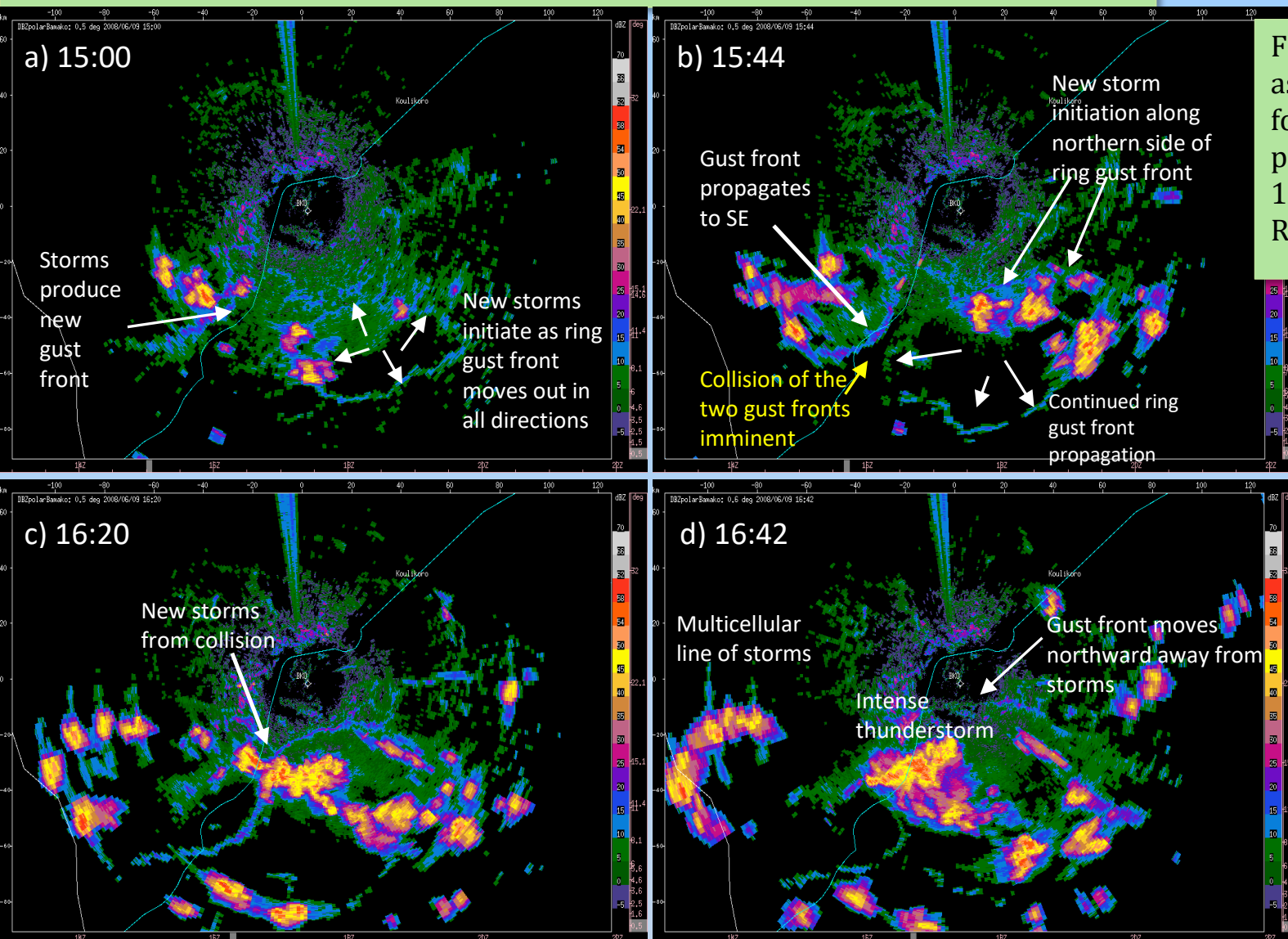


Figure 6.32. Same as Figure 6.30, but for four later time periods from 1500-1642 UTC. (Source: R. Roberts, 2014)

Meteorology of Tropical West Africa: The Forecasters' Handbook

Chapter 6: Nowcasting – Authors: Rita D. Roberts and James W. Wilson

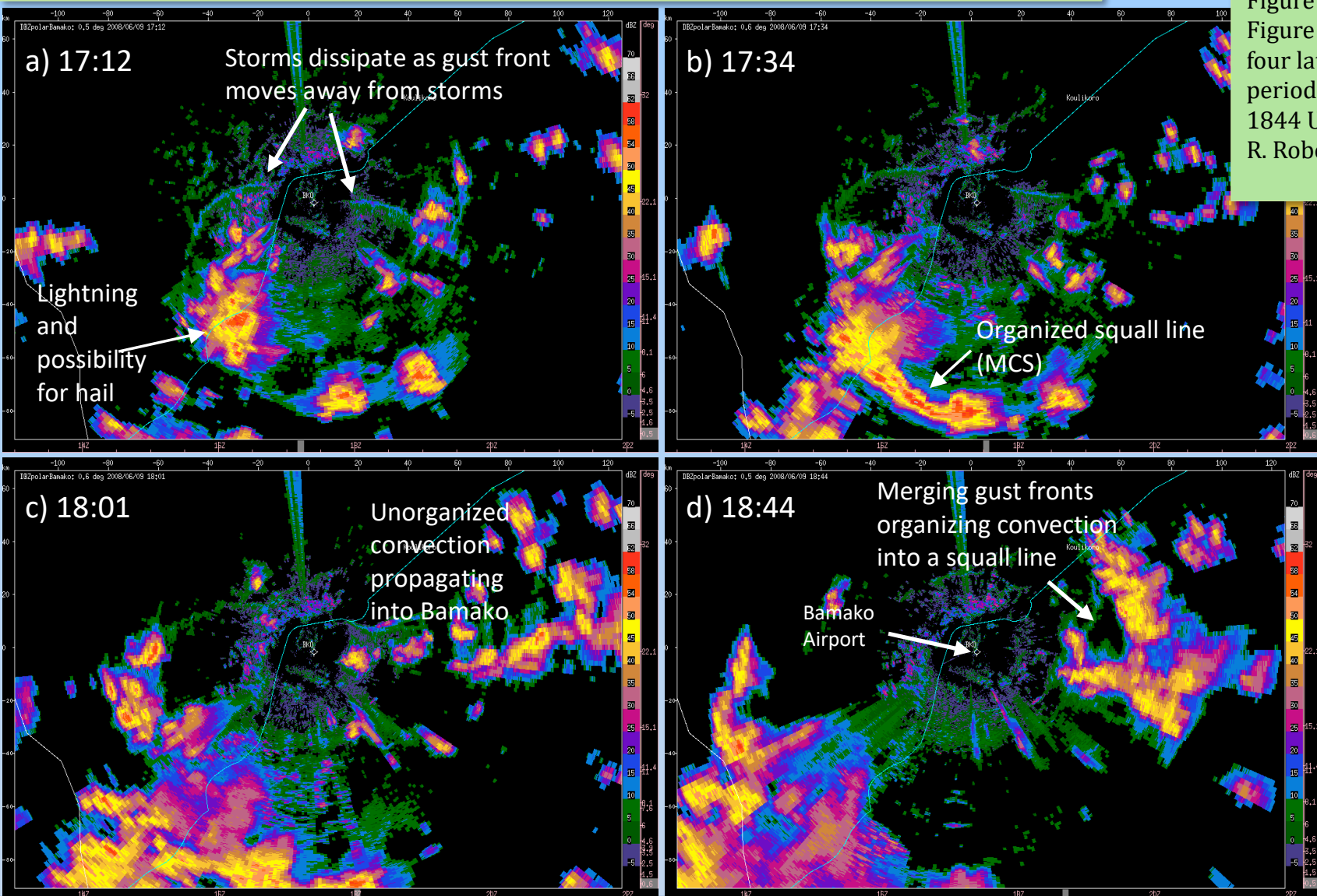


Figure 6.33. Same as Figure 6.32 but for four later time periods from 1712-1844 UTC. (Source: R. Roberts, 2014)

Meteorology of Tropical West Africa: The Forecasters' Handbook

Chapter 6: Nowcasting – Authors: Rita D. Roberts and James W. Wilson

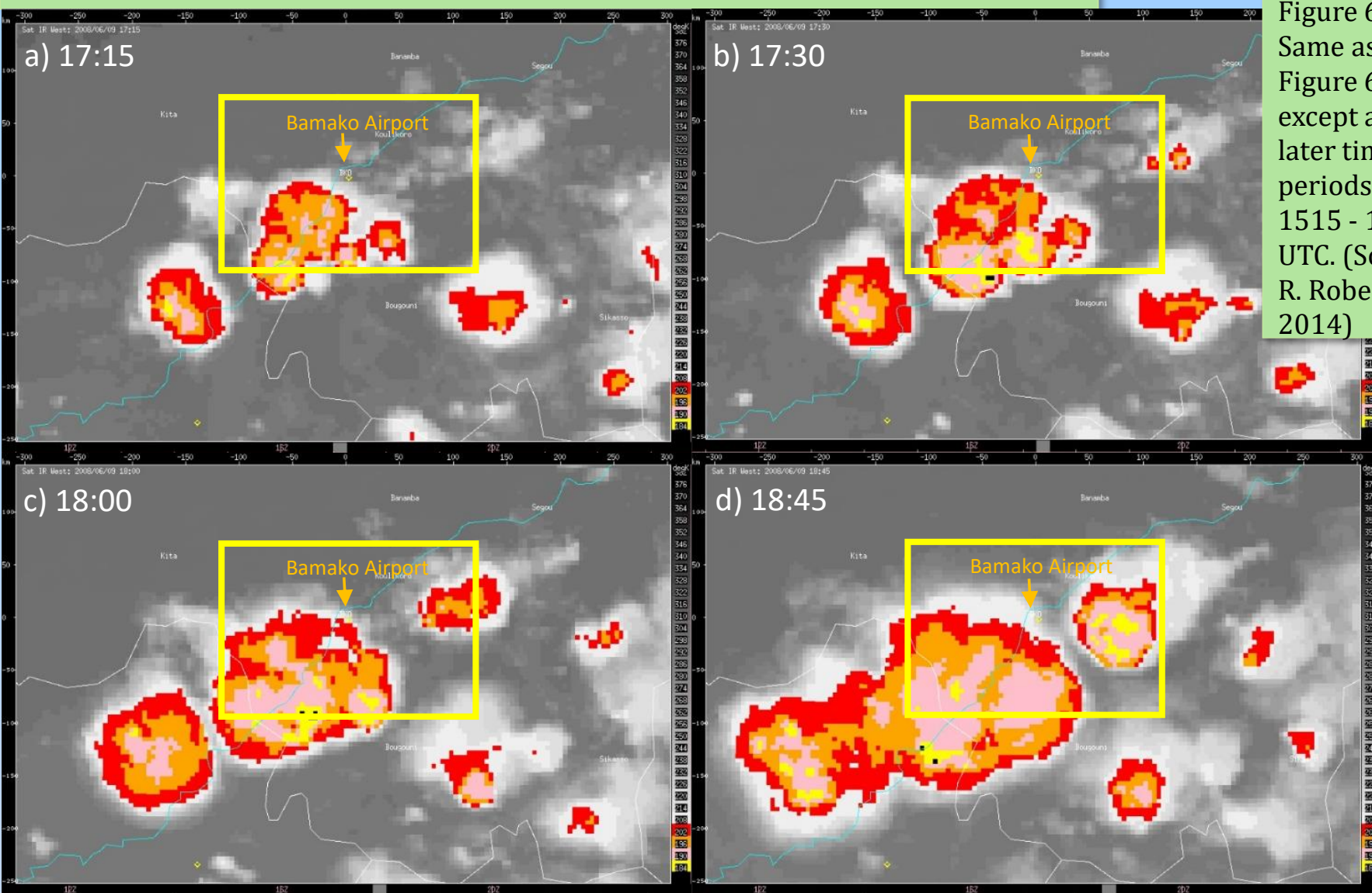
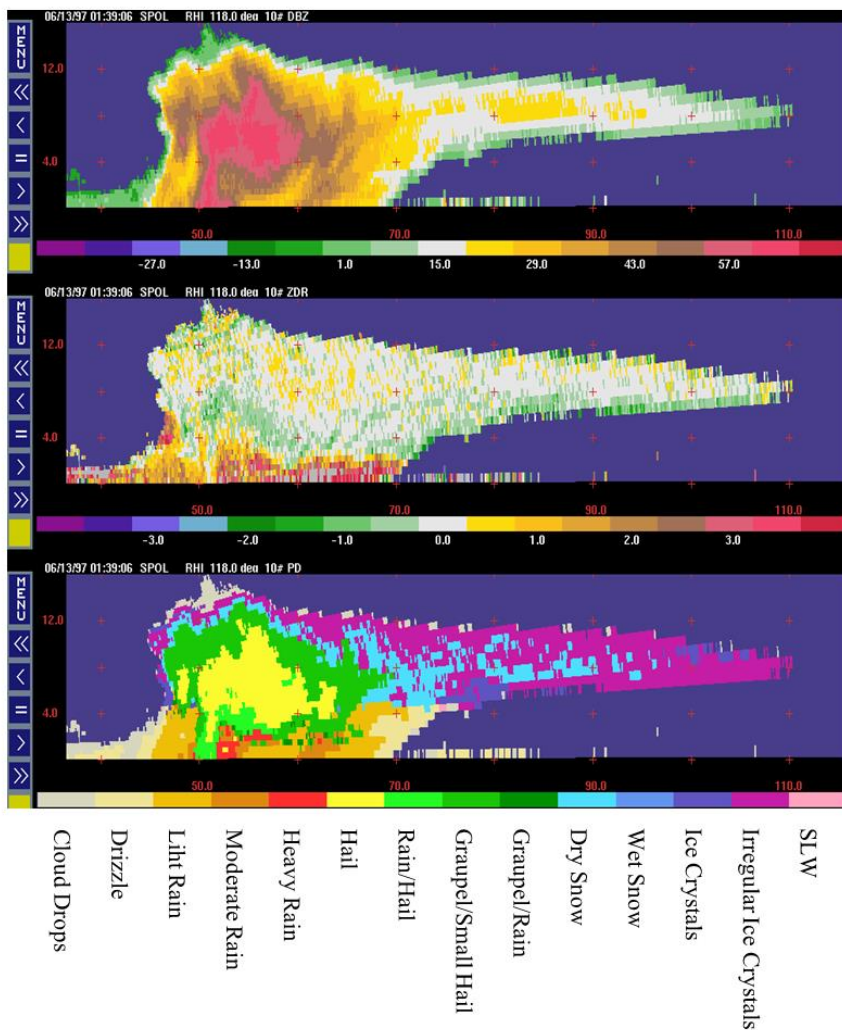


Figure 6.34. Same as Figure 6.31, except at four later time periods from 1515 - 1845 UTC. (Source: R. Roberts, 2014)



RHI scans of Z, ZDR and the corresponding particle classification results. The radar measurements were collected by NCAR S-Pol radar during the CASES 97 field program.

Figure 6.35. Range-Height Indicator (RHI) scans of reflectivity (top panel), differential reflectivity (ZDR; middle panel), and corresponding particle classification (PID) results. Measurements were collected by the NCAR S-Pol research radar in 1997. (Source: Vivekanandan et al., 1999)

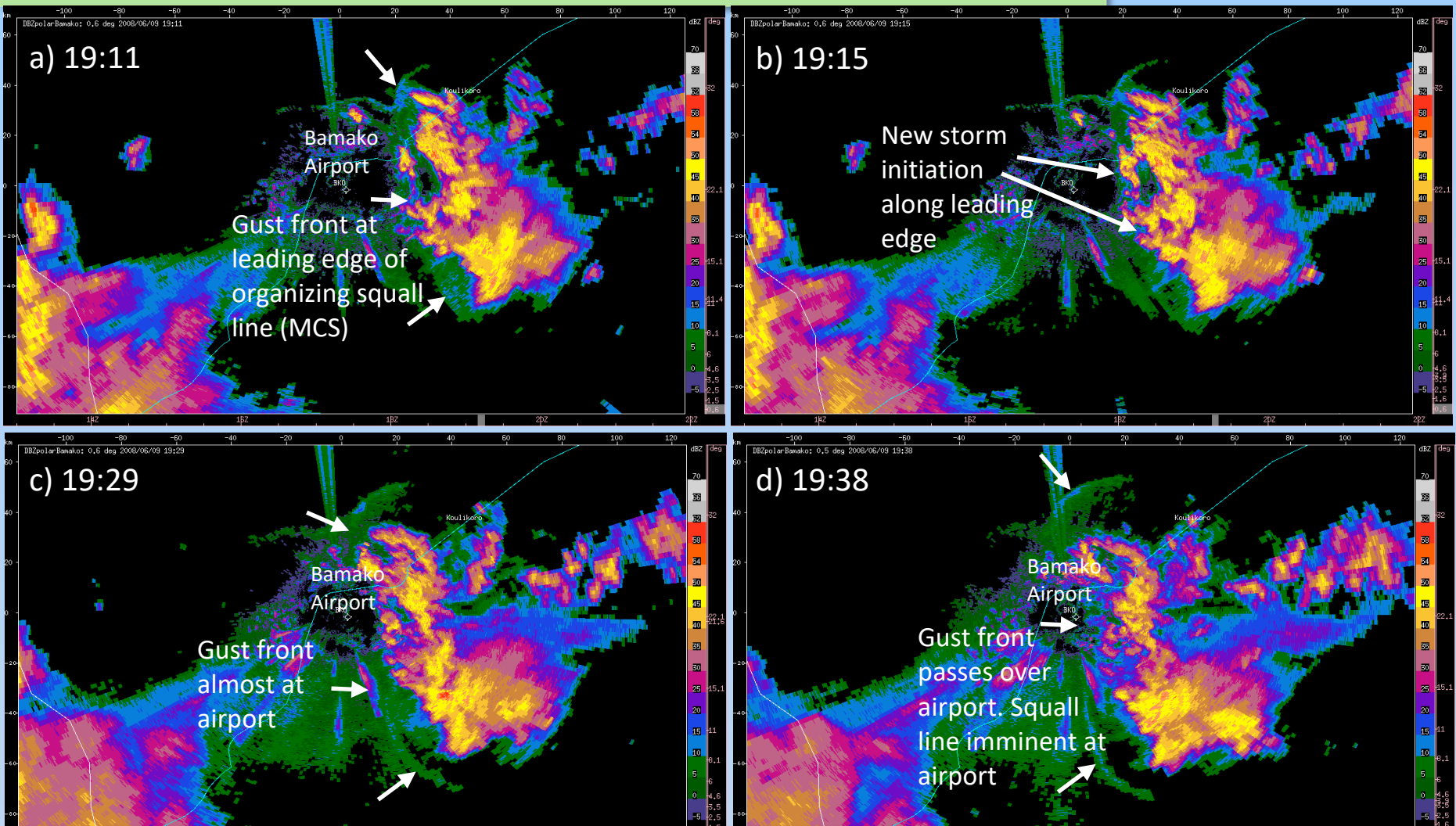
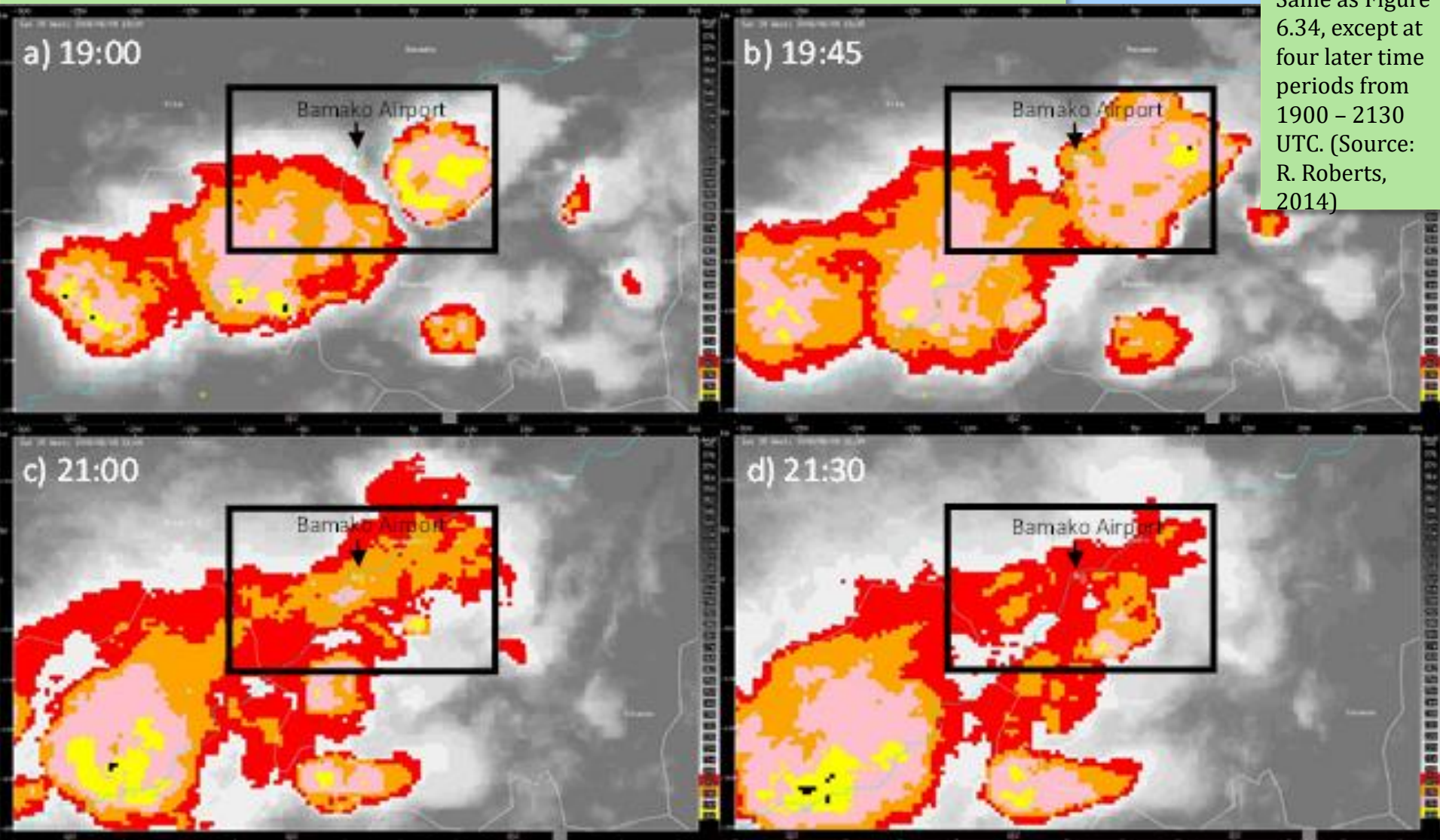


Figure 6.36. Same as Figure 6.33 but for four later time periods from 1911-1938 UTC. Small white arrows show leading edges of gust fronts. (Source: R. Roberts, 2014)

Meteorology of Tropical West Africa: The Forecasters' Handbook

Chapter 6: Nowcasting – Authors: Rita D. Roberts and James W. Wilson

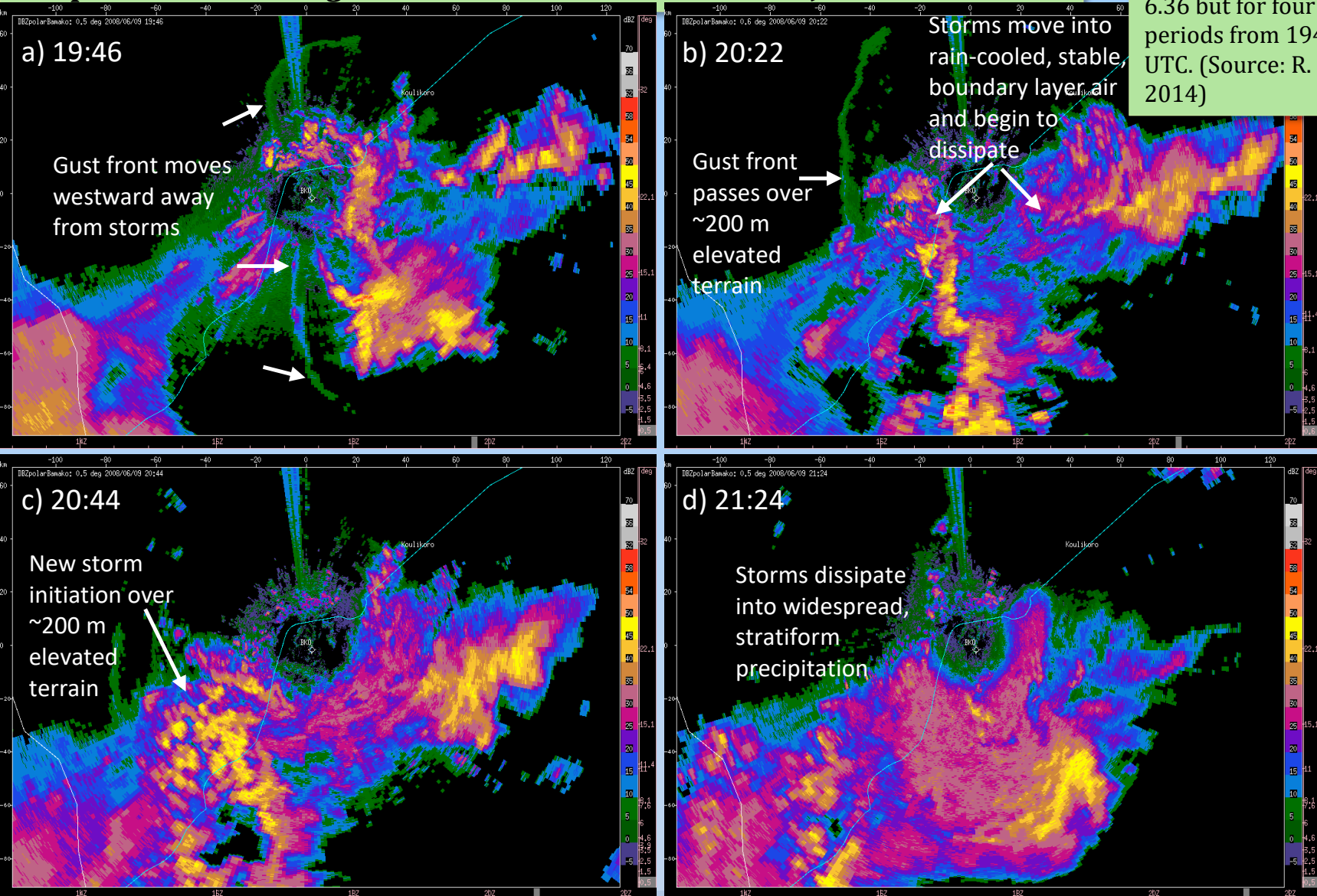
Figure 6.37.
Same as Figure 6.34, except at four later time periods from 1900 – 2130 UTC. (Source: R. Roberts, 2014)



Meteorology of Tropical West Africa: The Forecasters' Handbook

Chapter 6: Nowcasting – Authors: Rita D. Roberts and James W. Wilson

Figure 6.38. Same as Figure 6.36 but for four later time periods from 1946-2124 UTC. (Source: R. Roberts, 2014)



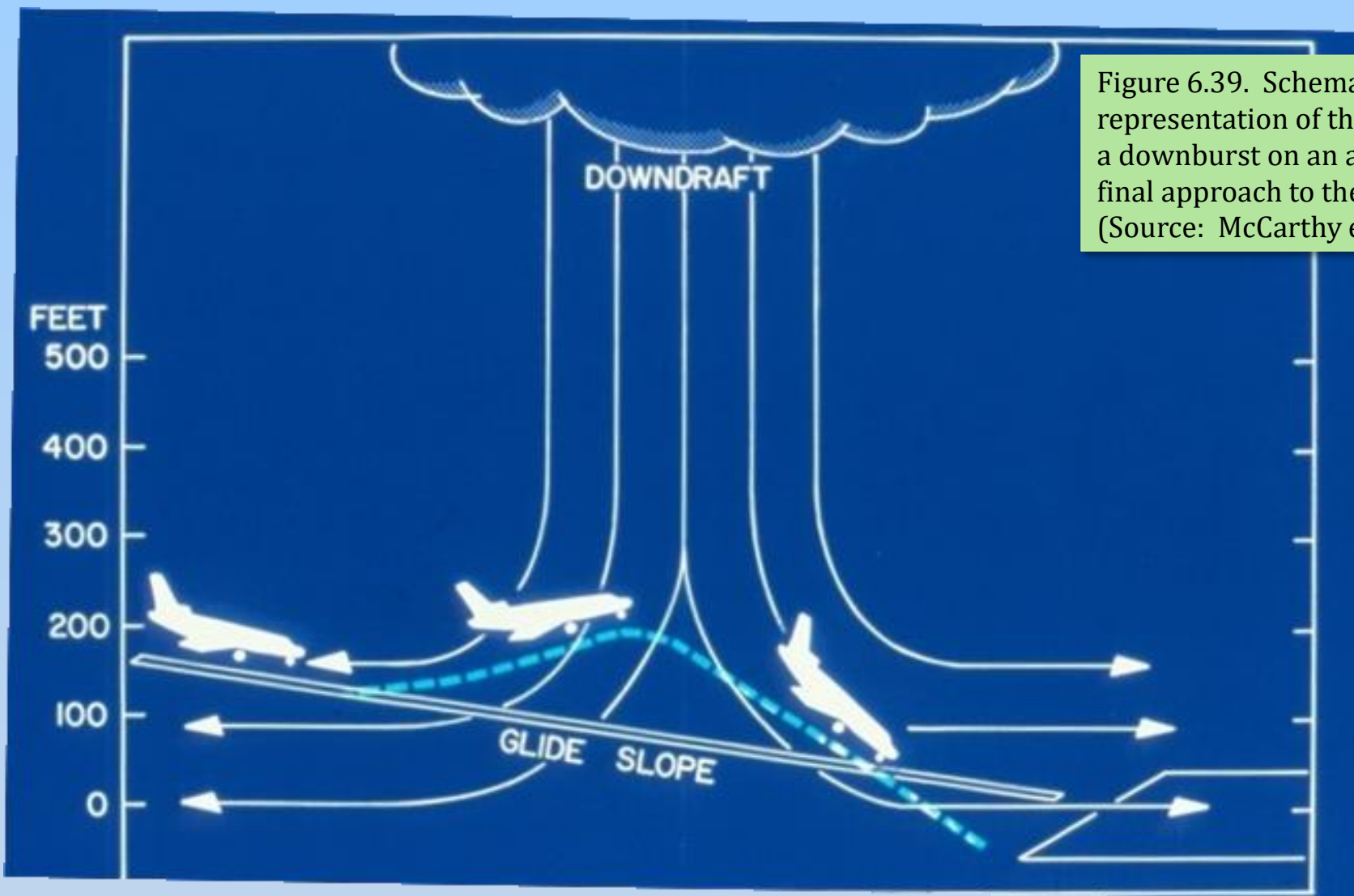


Figure 6.39. Schematic representation of the impact of a downburst on an aircraft on final approach to the runway. (Source: McCarthy et al., 1982)

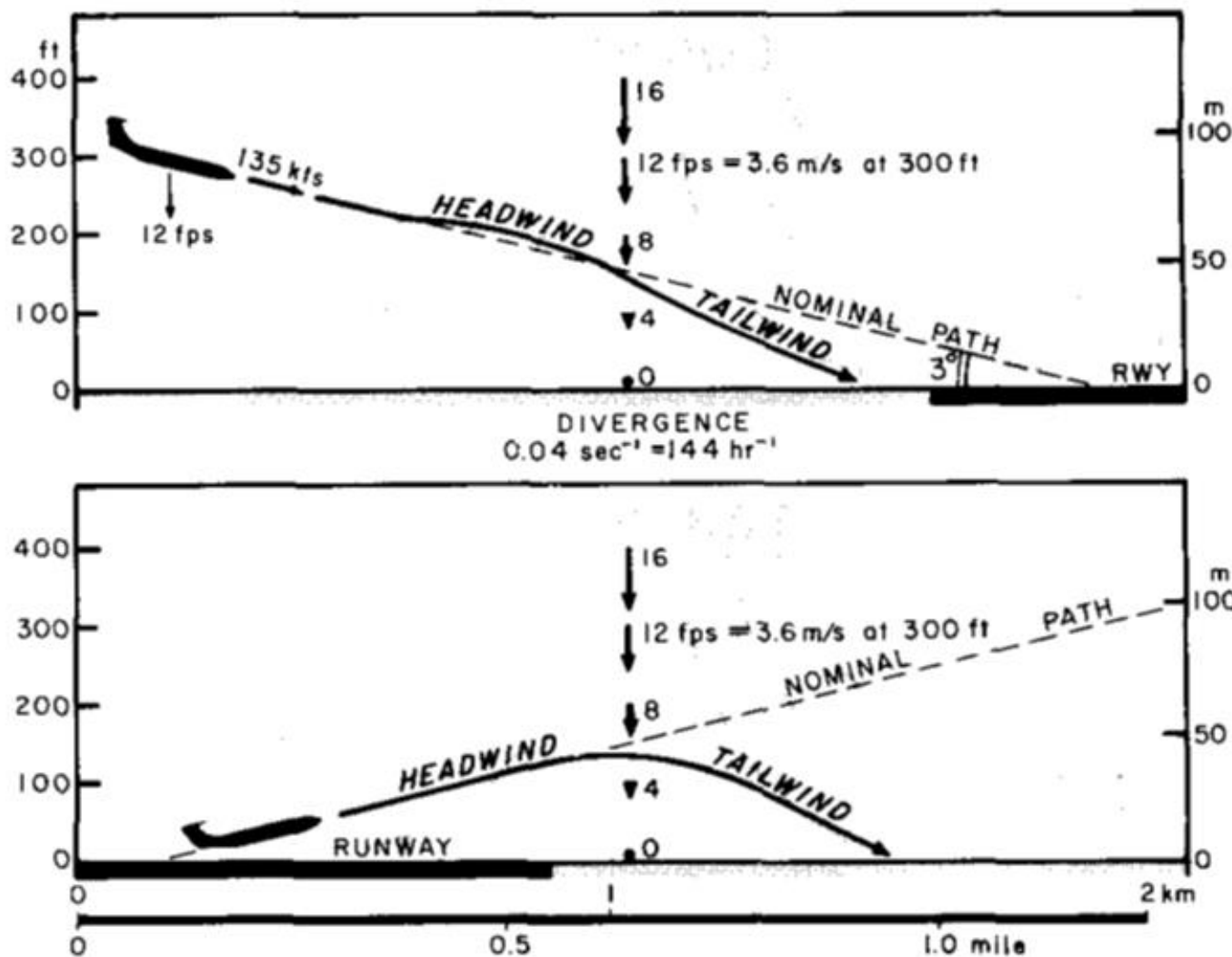
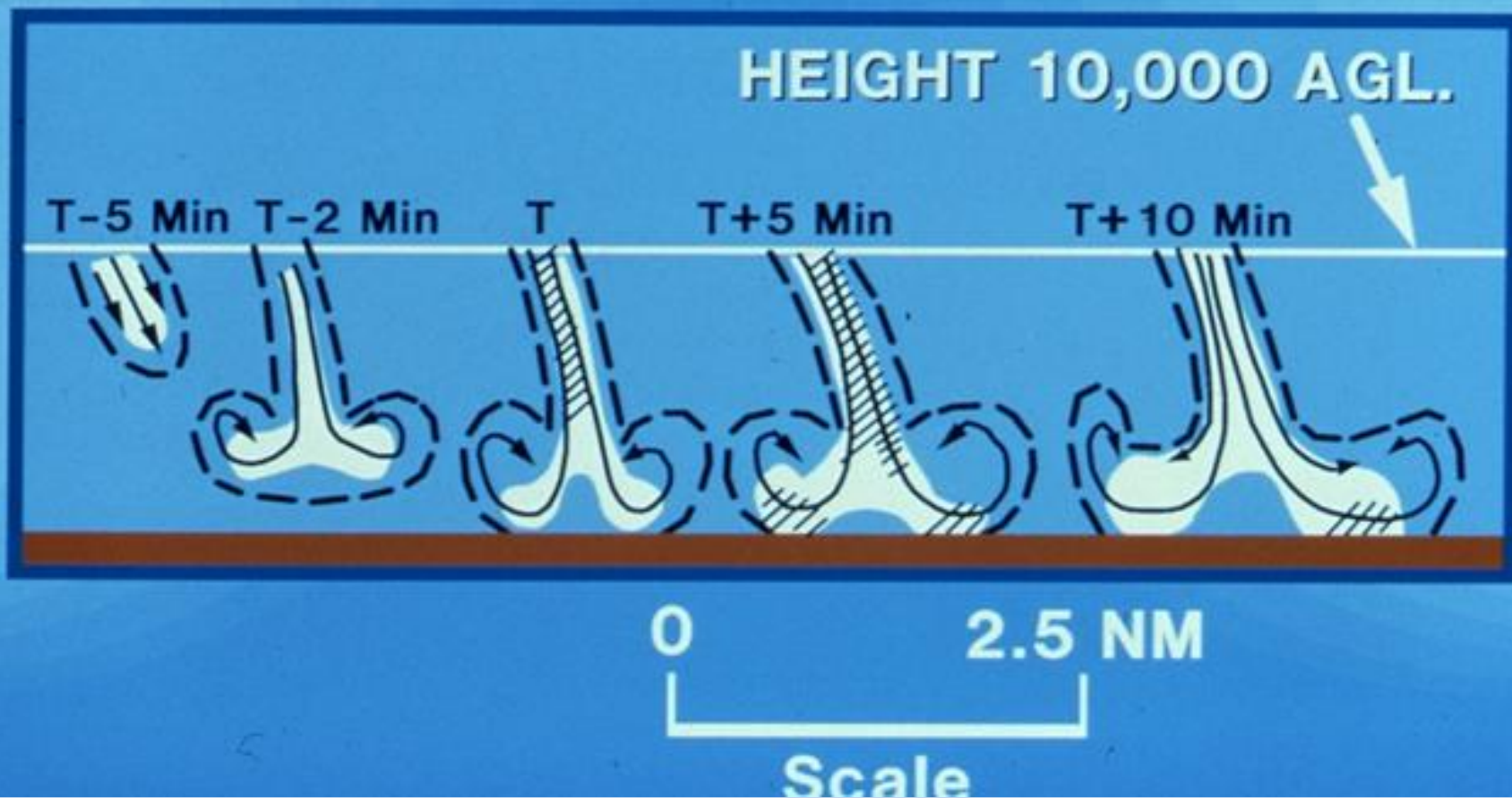


Figure 6.40. Schematic diagrams of flight paths under the influence of a downburst cell. Downward arrows represent downdraft with speeds of 3.6 ms^{-1} at an altitude of $<100 \text{ m}$ (300 ft). (Source: Fujita and Caracena, 1977)

Figure 6.41. Schematic representation of the short-lived, temporal evolution and very small spatial scale of a microburst occurring below 3000 m (10,000 ft.). Scale is in nautical miles. (Source: Wilson et al., 1984;



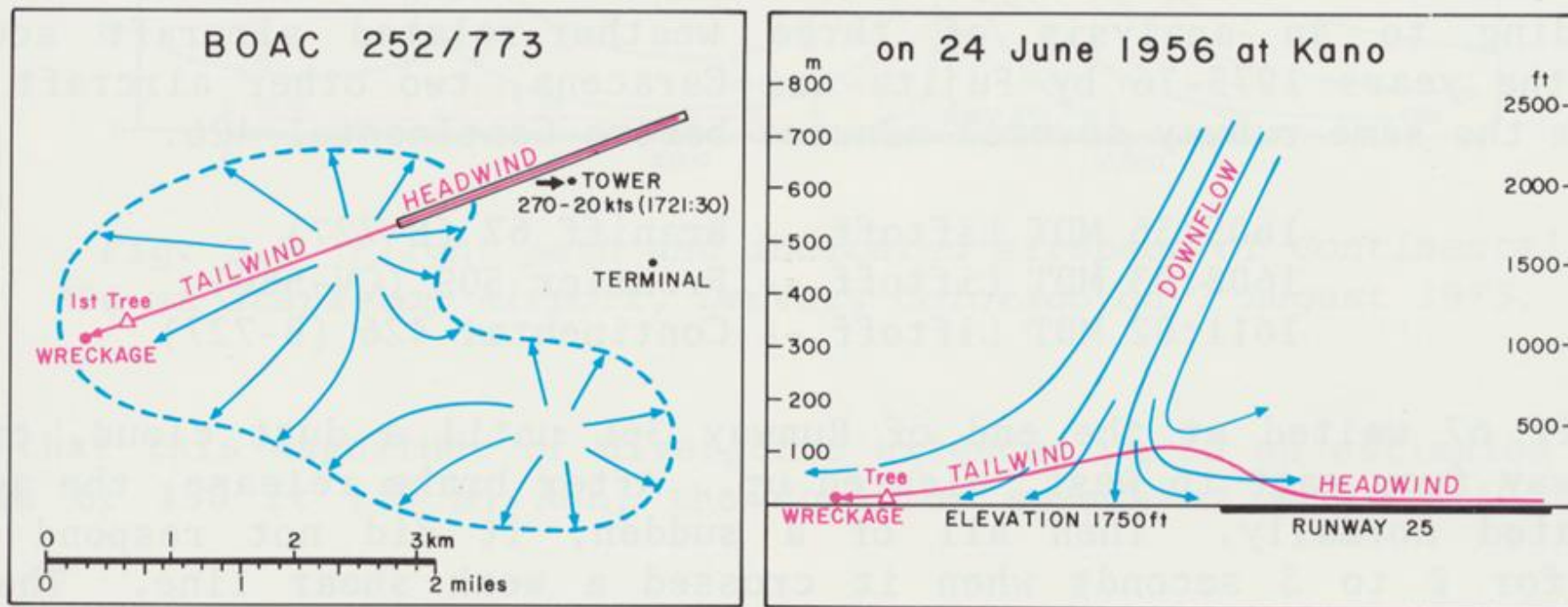


Figure 6.42. Vertical and horizontal views of the microburst that caused the crash of BOAC Flight 252/773 accident at Kano, Nigeria. Wind patterns were reconstructed based on observations and information received from the Ministry of Transport and Civil Aviation, HMSO, London, U.K. (Source: Fujita, 1985).

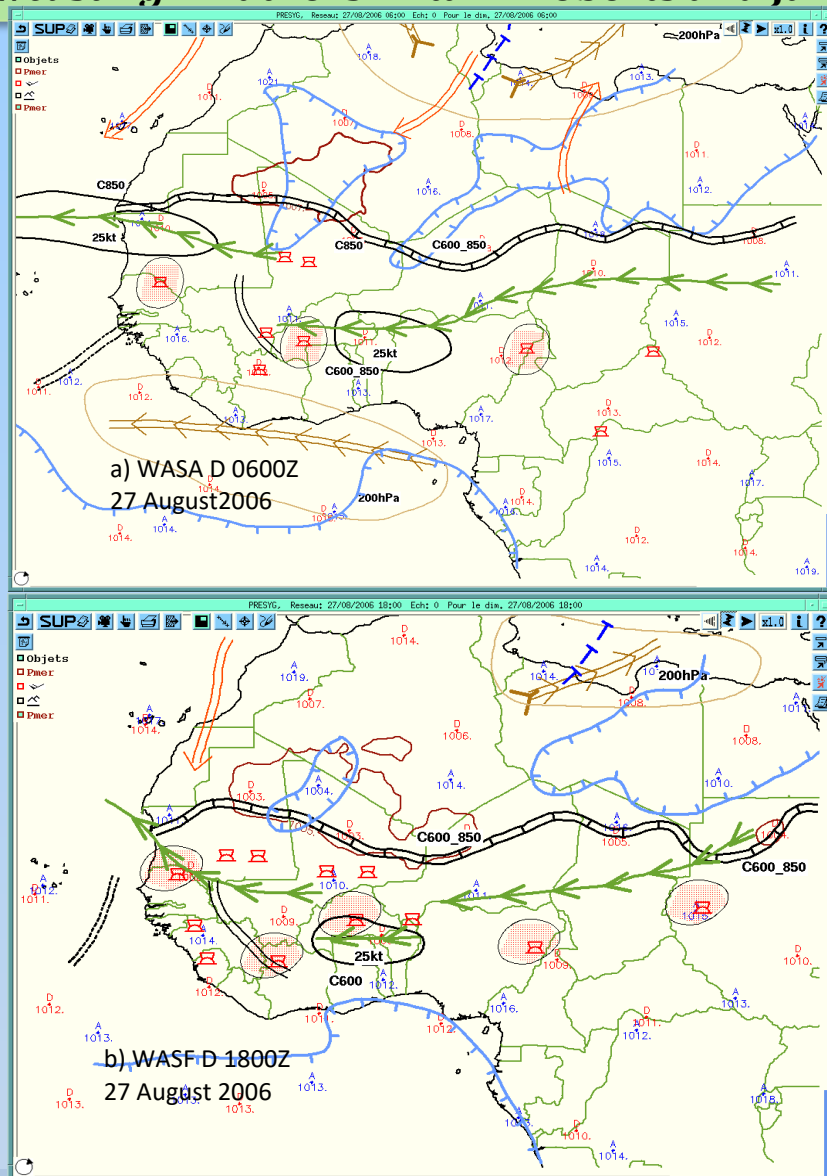


Figure 6.43. Weather analysis (WASA) and forecast (WASF) maps for 27 August 2006 over Western Africa. Shown are the inter-tropical discontinuity (ITD) (double-black barred contours); the African Easterly Jet (AEJ) locations (green line contours with arrowheads); the African Easterly Waves trough (AEW; double-black contours); the subtropical jet (orange double-line contours with arrowheads); shaded polygons representing areas of most intense convection (MCS) estimated from the IR imagery (orange corresponding to -65°C); and isolated convective cells (identified by a Cb symbol only). See Chapter 12 for further explanations. (a) WASA at 0600 UTC and (b) WASF for 1800 UTC. (Source: Meteo-France, 2014)

Meteorology of Tropical West Africa: The Forecasters' Handbook

Chapter 6: Nowcasting - Authors: Rita D. Roberts and James W. Wilson

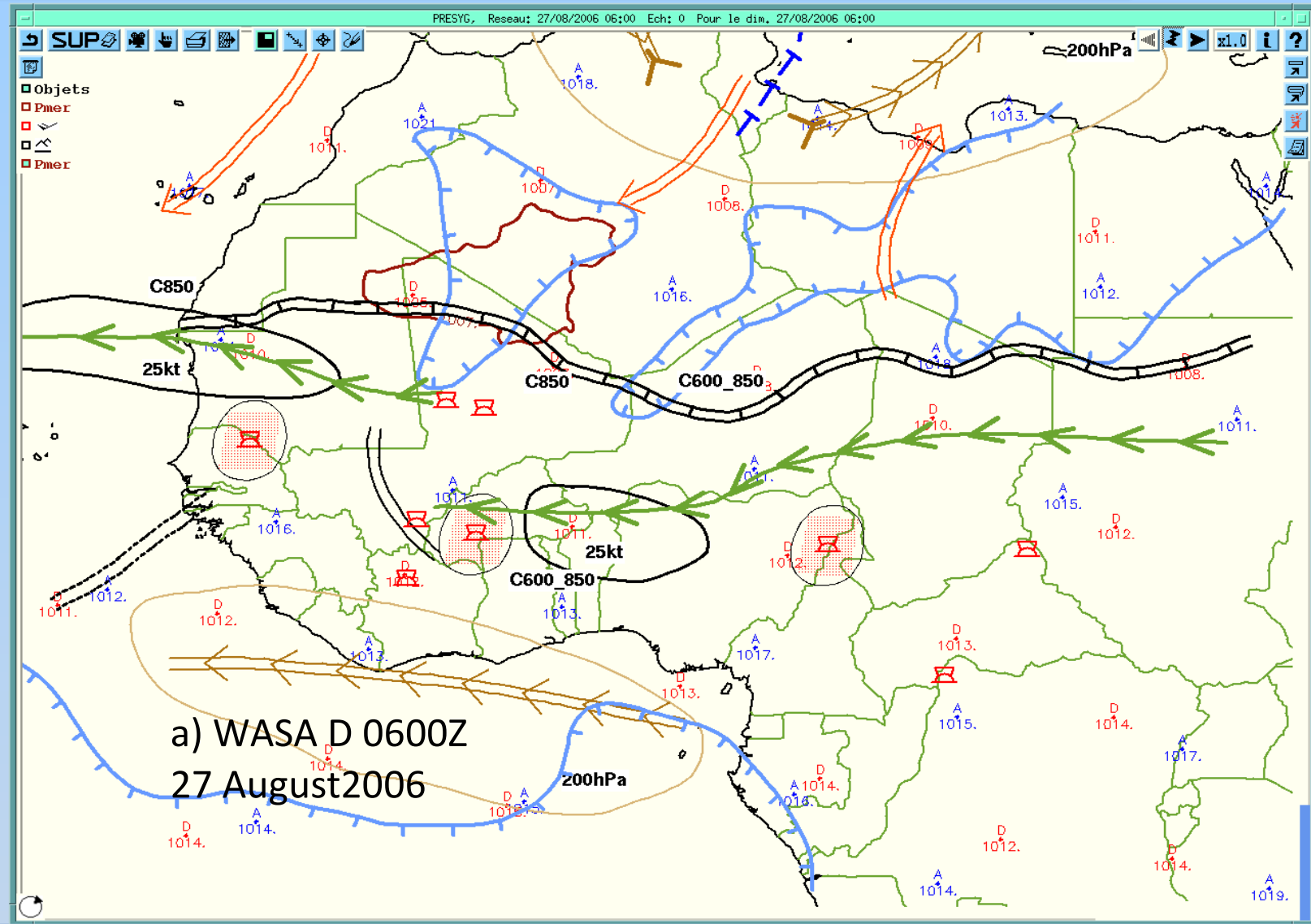


Figure 6.43. Weather analysis (WASA) and forecast (WASF) maps for 27 August 2006 over Western Africa.

Meteorology of Tropical West Africa: The Forecasters' Handbook

Chapter 6: Nowcasting – Authors: Rita D. Roberts and James W. Wilson

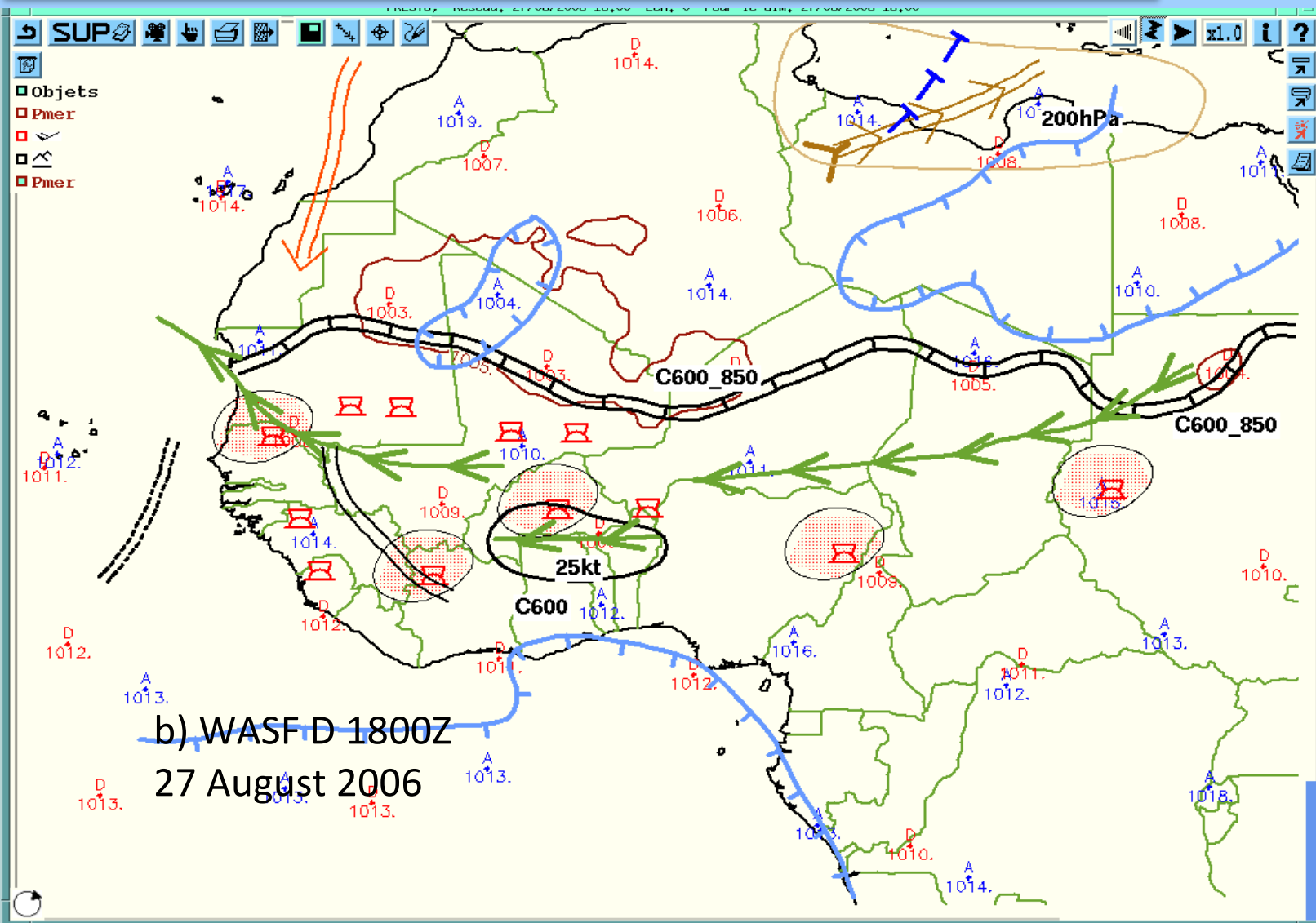


Figure 6.43. Weather analysis (WASA) and forecast (WASF) maps for 27 August 2006 over Western Africa.

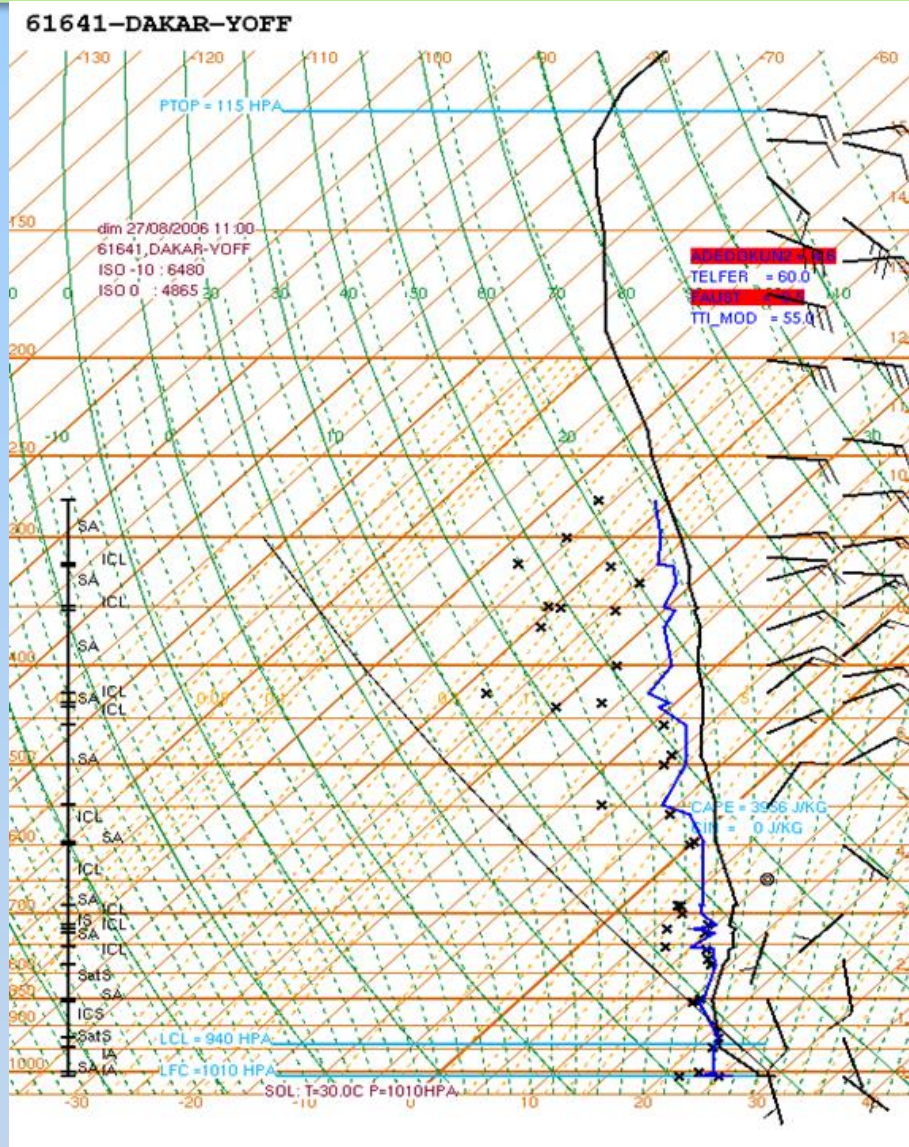


Figure 6.44. Tephigram sounding at 11:00 UTC on 27 August 2006 for Dakar, Senegal. Sounding calculated values for CAPE and CIN were 3956 J/KG and 0 J/KG, respectively. (Source: AMMA Experiment web site, 2014)

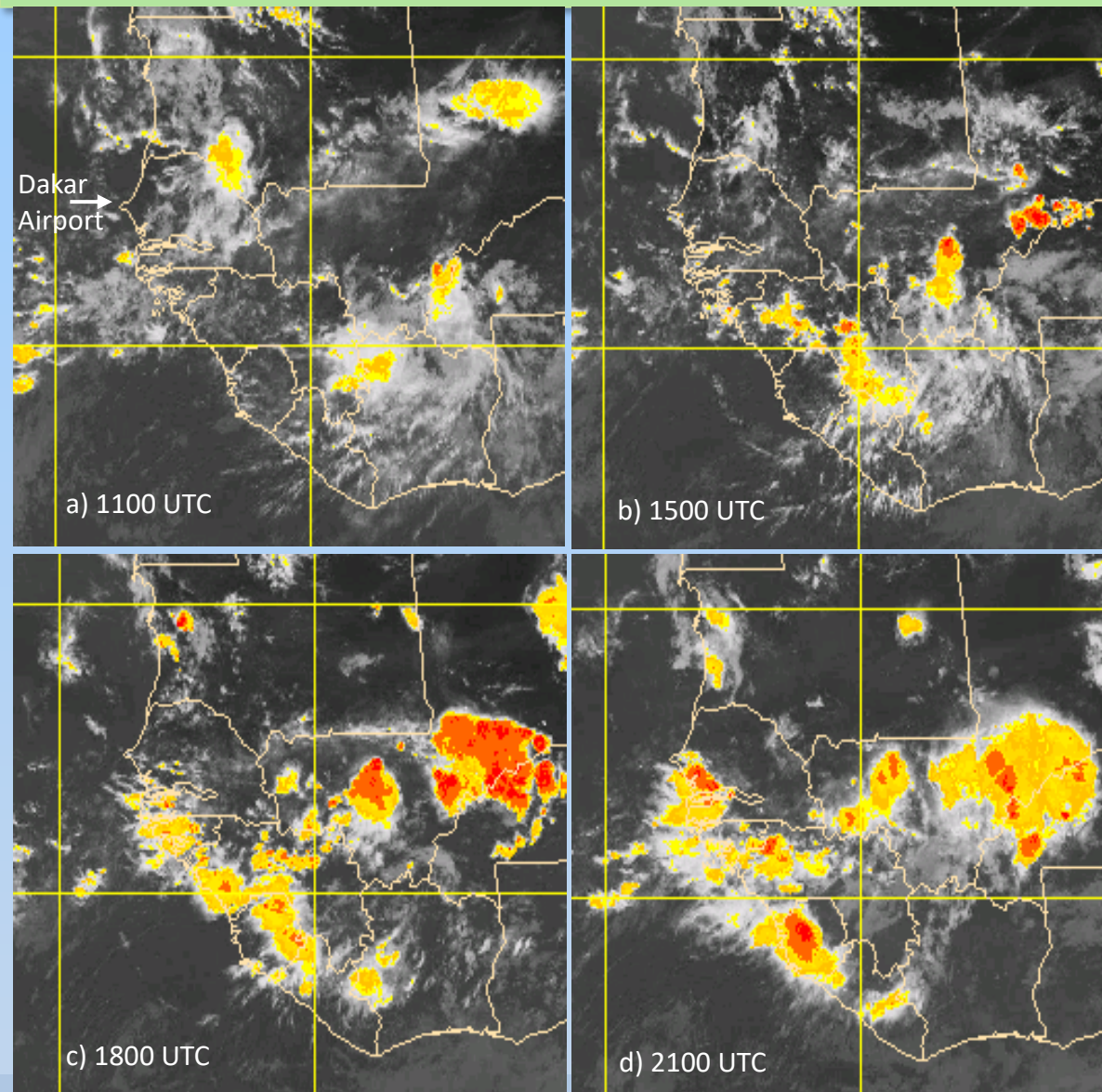


Figure 6.45. Meteosat Infrared (10.8 micron) imagery on 27 August 2006 at a) 1100 UTC, b) 1500 UTC, c) 1800 UTC, and d) 2100 UTC. Orange areas represent cloud-top temperatures of -65°C used for tracking intense MCSs. The approximate location of the Dakar, Senegal airport is indicated in (a). (Source: AMMA Experiment web site, 2014)

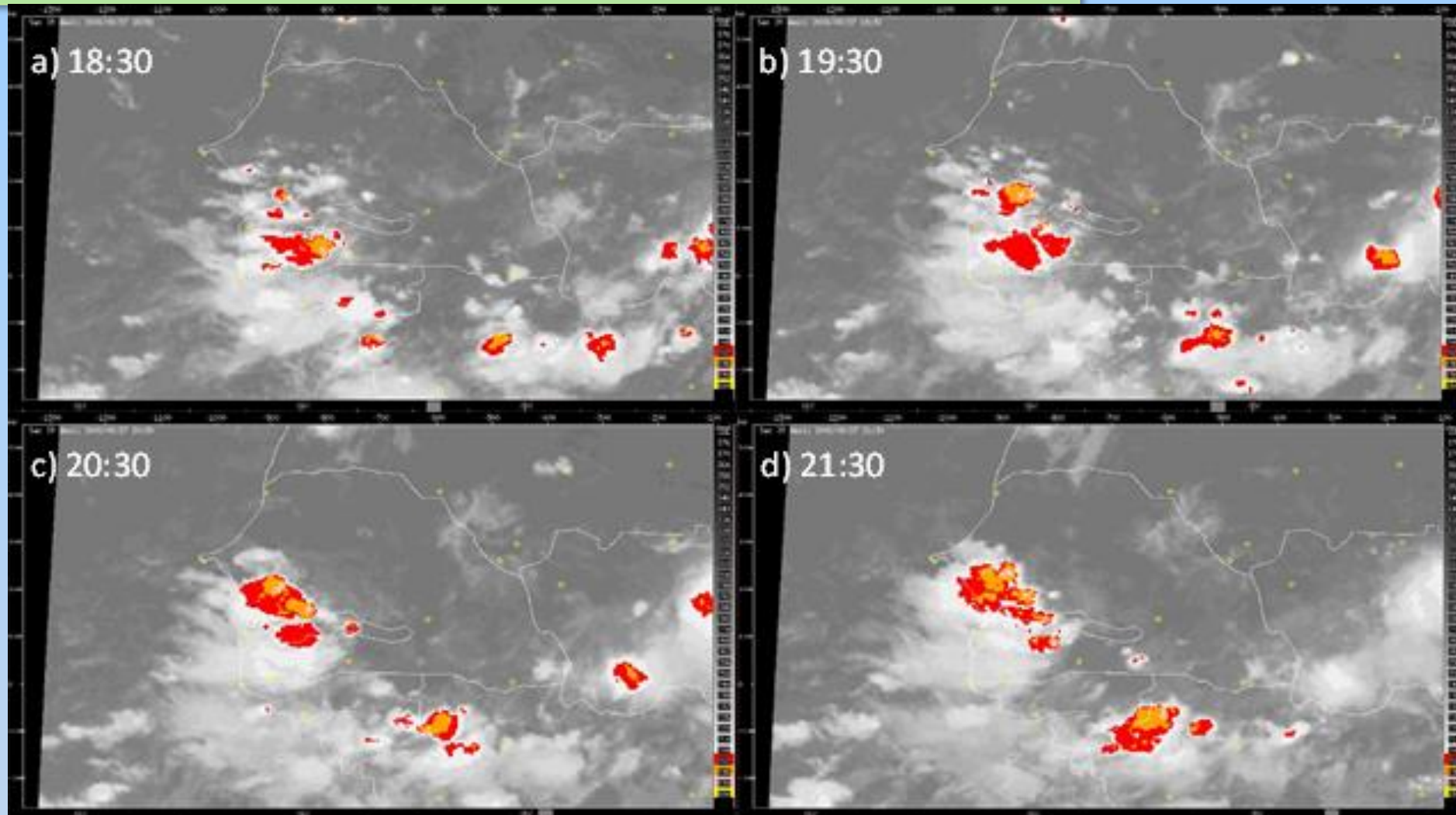


Figure 6.46. Sequence of satellite infrared imagery from 1830-2130 UTC centered on Senegal. Orange shades represent cloud- top temperatures colder than -67°C . Country borders are outlined in white. (Source: R. Roberts, 2014)

Chapter 6: Nowcasting – Authors: Rita D. Roberts and James W. Wilson

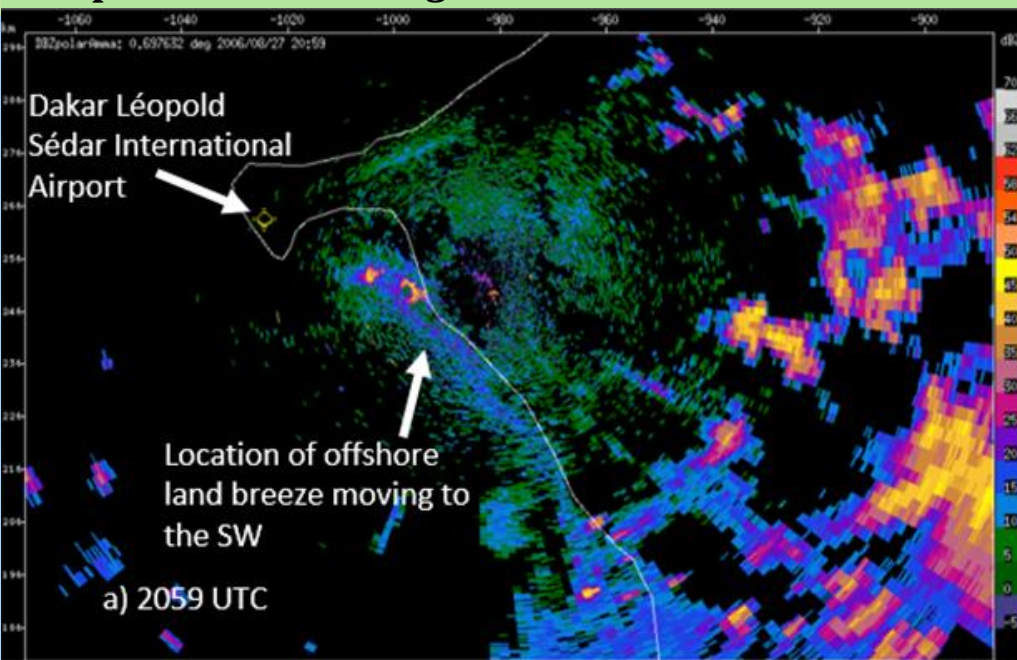
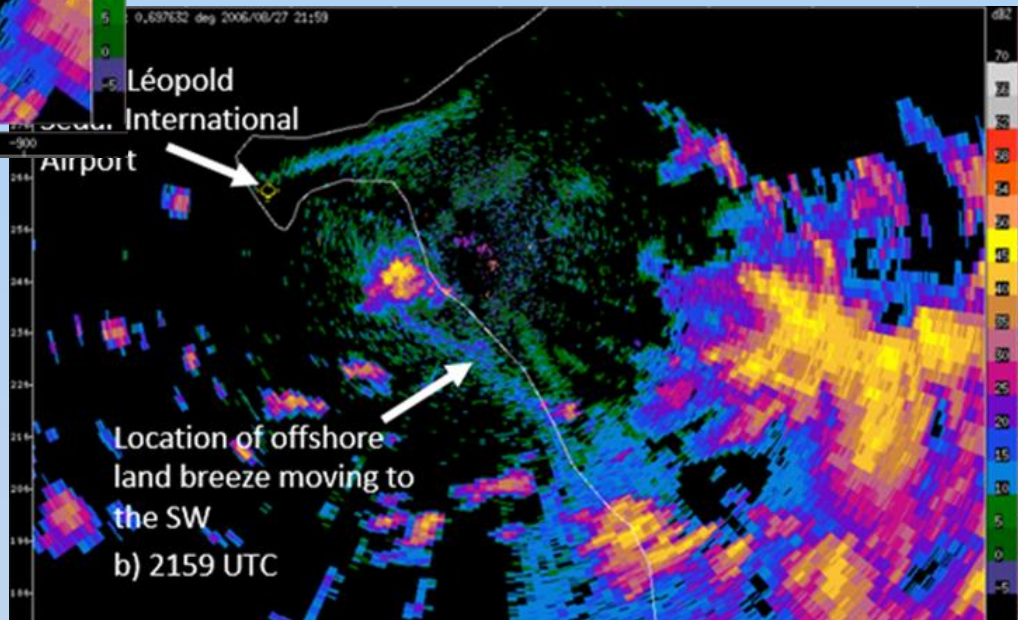


Figure 6.47. NASA NPOL radar reflectivity image at 2059 UTC on 27 August 2006. The white contour is the coastline of Senegal and the yellow icon represents the location of the Dakar Airport. The radar is located 40 km to the SE of the airport. (a) 2059 UTC; (b) 2159 UTC. (Source: R. Roberts, 2014)



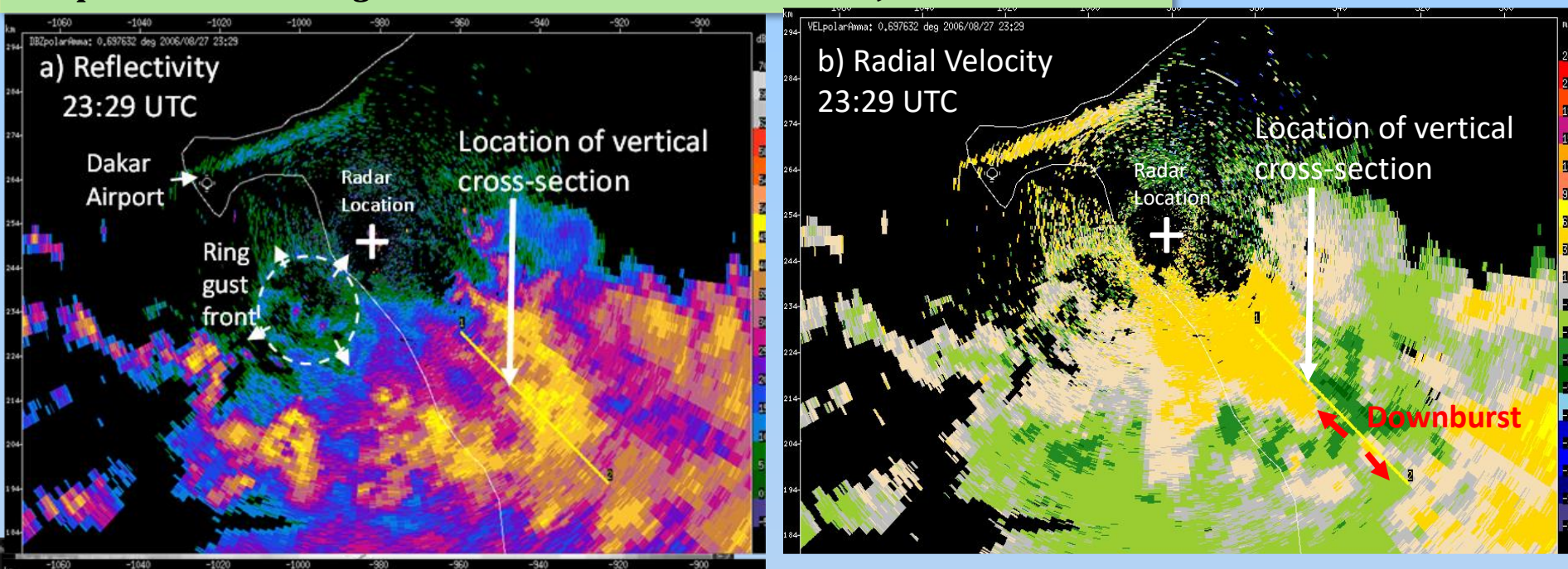
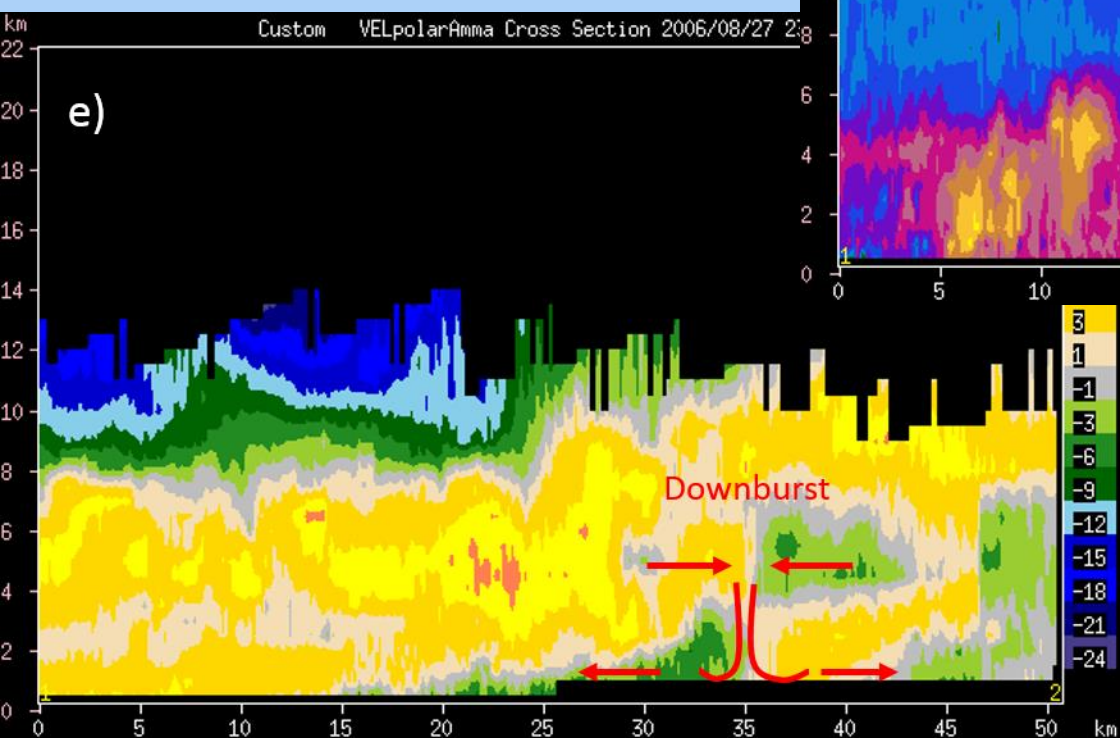
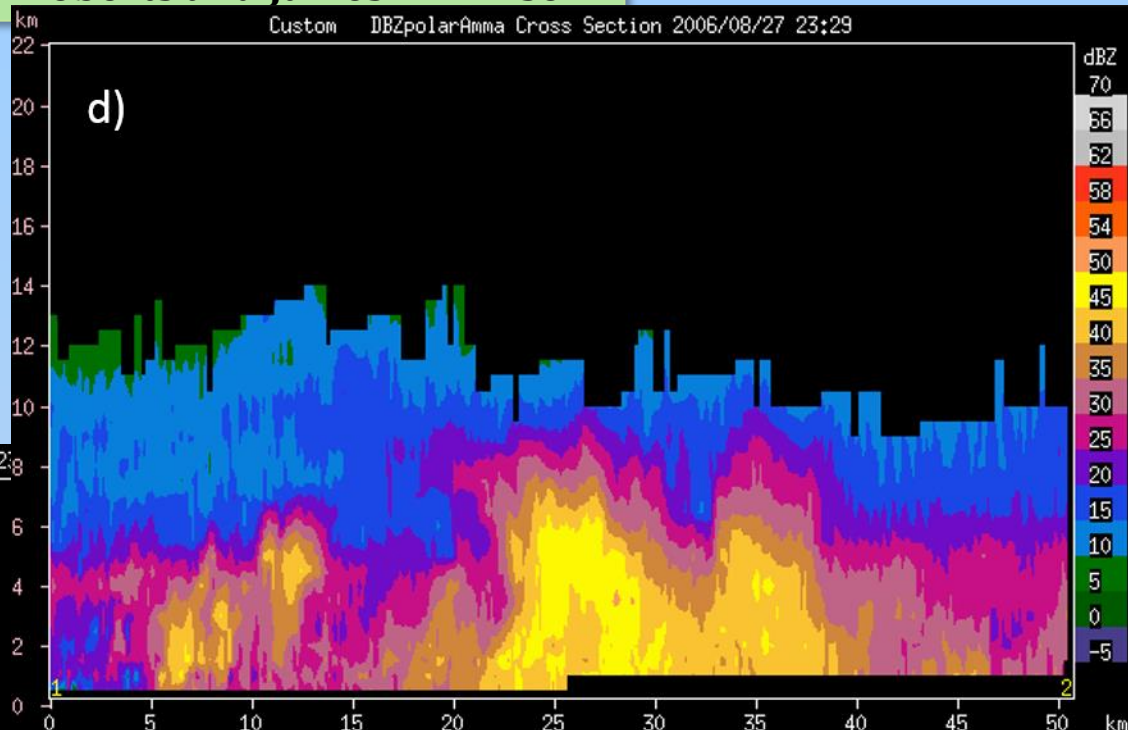


Figure 6.48. Radar horizontal and vertical cross-sections through a downburst-producing storm in Senegal on 27 August 2006 at 2329 UTC. a) Horizontal radar reflectivity (in dBZ units). Higher reflectivity values represent more intense storms and precipitation. b) Horizontal radar radial velocity (in ms-1). Blue and green shades are regions of flow toward the radar, and yellow and red shades are flow away from the radar. Yellow line shows the locations of vertical cross-sections shown in d) and e), next slide. The red arrows in b) show the Doppler wind directions associated with the downburst. c) Satellite IR image at 2330 UTC. Orange shade is -67°C and pink shade is -88°C . (Source: R. Roberts, 2014)

Meteorology of Tropical West Africa: The Forecasters' Handbook

Chapter 6: Nowcasting – Authors: Rita D. Roberts and James W. Wilson

Figure 6.48 cont'd. d,e) Radar reflectivity (vertical) cross-section (in dBZ). e) Radar radial velocity (vertical) cross-section (in ms⁻¹). Blue and green shades are regions of flow toward the radar, and yellow and red shades are flow away from the radar. Radar position is located to the left of the image. (Source: R. Roberts, 2014)



Meteorology of Tropical West Africa: The Forecasters' Handbook

Chapter 6: Nowcasting – Authors: Rita D. Roberts and James W. Wilson

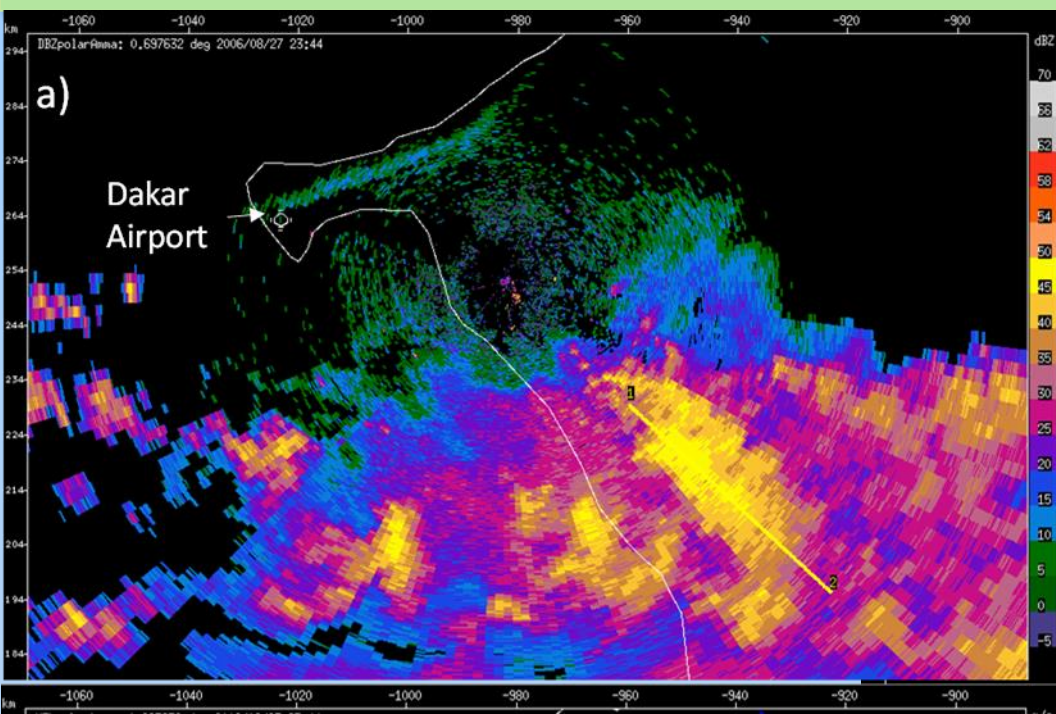
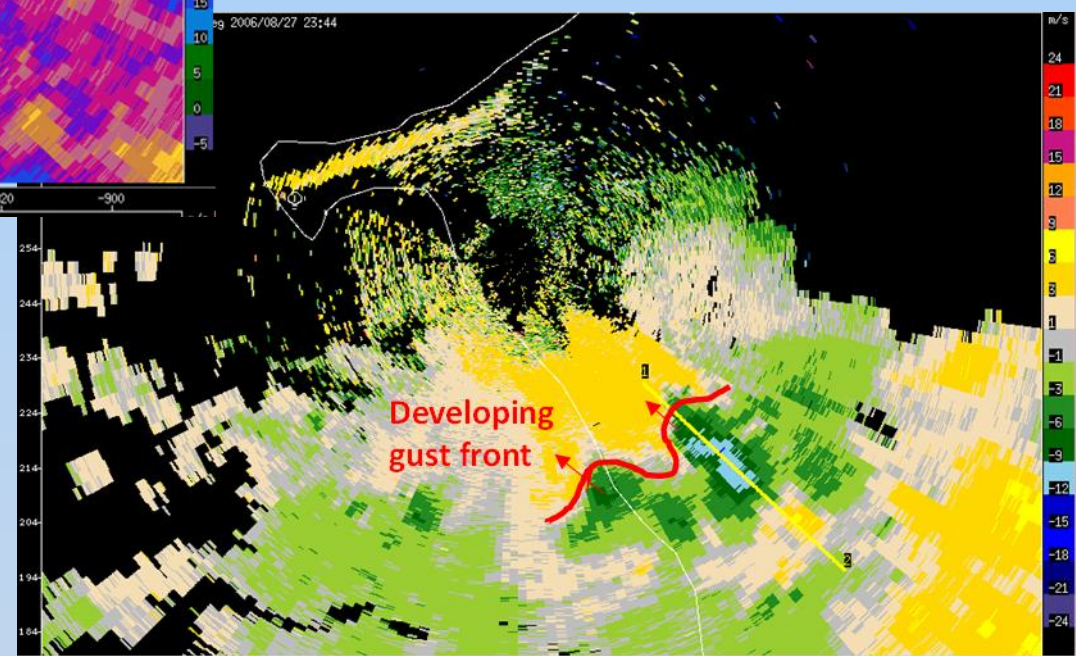


Figure 6.49. Radar horizontal and vertical cross-sections through a downburst-producing storm in Senegal on 27 August 2006 at 2344 UTC. a) Horizontal radar reflectivity (in dBZ) and b) horizontal radar radial velocity (in ms⁻¹). Blue and green shades are regions of flow toward the radar, and yellow and red shades are flow away from the radar. Yellow line shows the location of the vertical cross-sections in c) and d), next slide. (Source: R. Roberts, 2014)



Chapter 6: Nowcasting – Authors: Rita D. Roberts and James W. Wilson

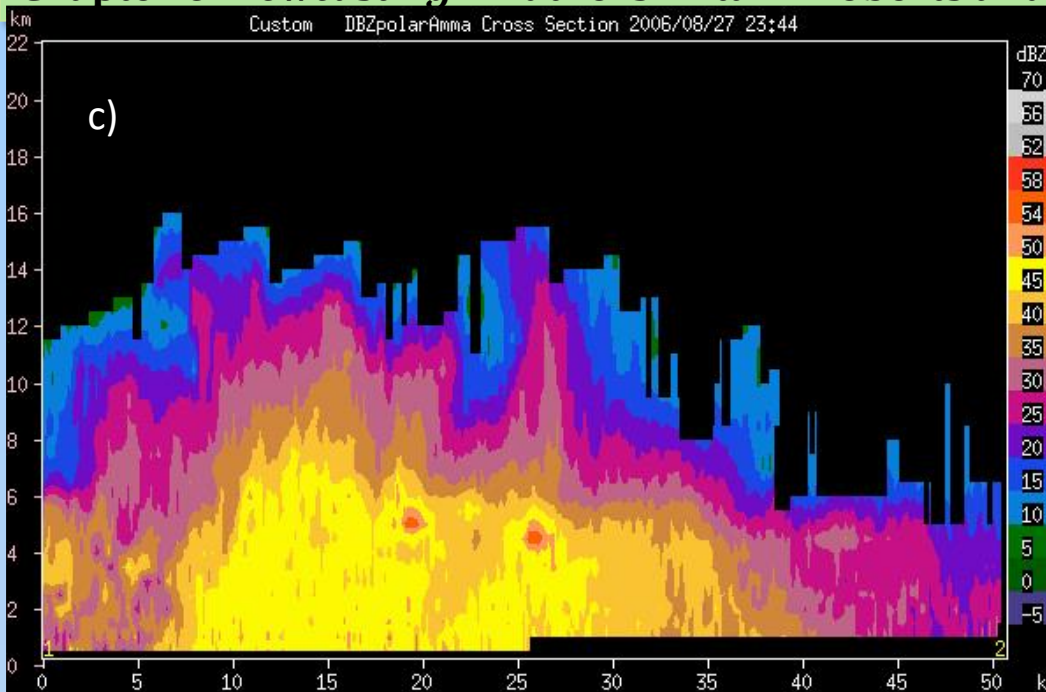
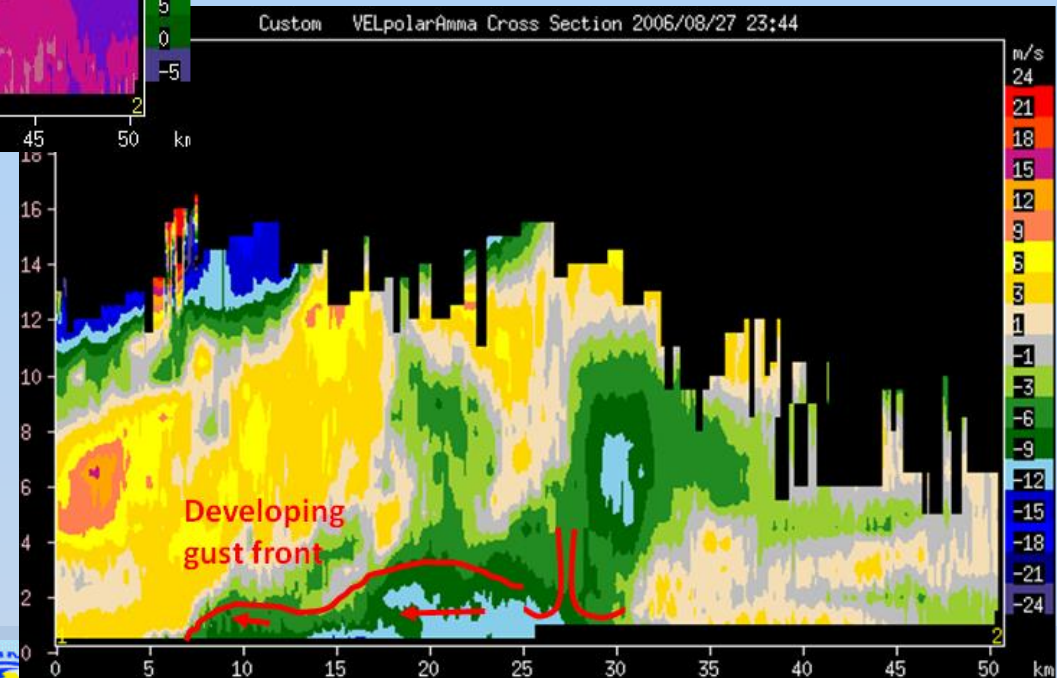


Figure 6.49 cont'd. c) Radar reflectivity (vertical) cross-section (in dBZ). d) Radar radial velocity (vertical) cross-section (in ms⁻¹). Blue and green shades are regions of flow toward the radar, and yellow and red shades are flow away from the radar. Radar position is located to the left of the image. (Source: R. Roberts, 2014)



Chapter 6: Nowcasting - Authors: Rita D. Roberts and James W. Wilson

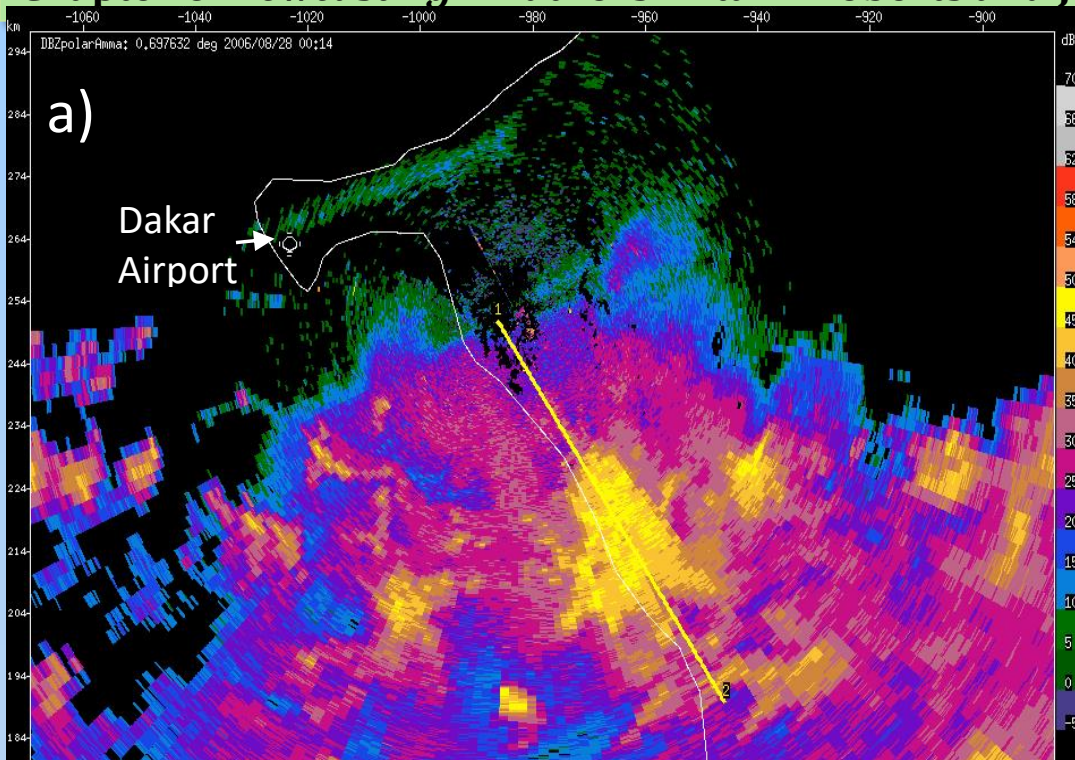
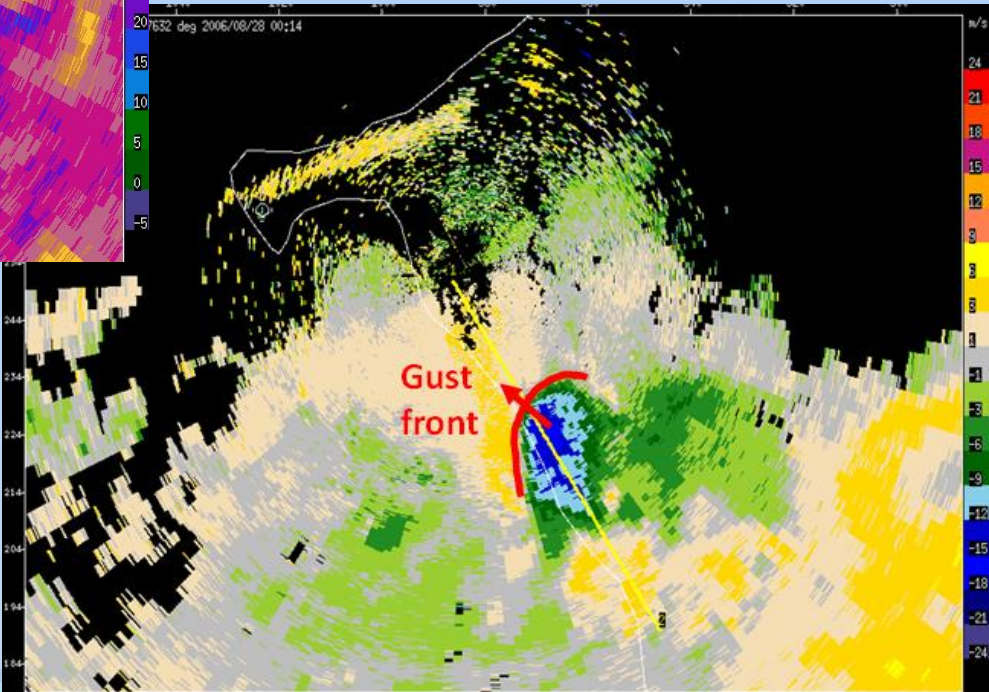


Figure 6.50. Radar horizontal and vertical cross-sections through a downburst-producing storm in Senegal on 27 August 2006 at 00:14 UTC. a) Horizontal radar reflectivity (in dBZ) and b) horizontal radar radial velocity (in ms⁻¹). (Source: R. Roberts, 2014)



Blue and green shades are regions of flow toward the radar, and yellow and red shades are flow away from the radar. Yellow line shows the location of the vertical cross-sections in c) and d), next slide.

Meteorology of Tropical West Africa: The Forecasters' Handbook

Chapter 6: Nowcasting – Authors: Rita D. Roberts and James W. Wilson

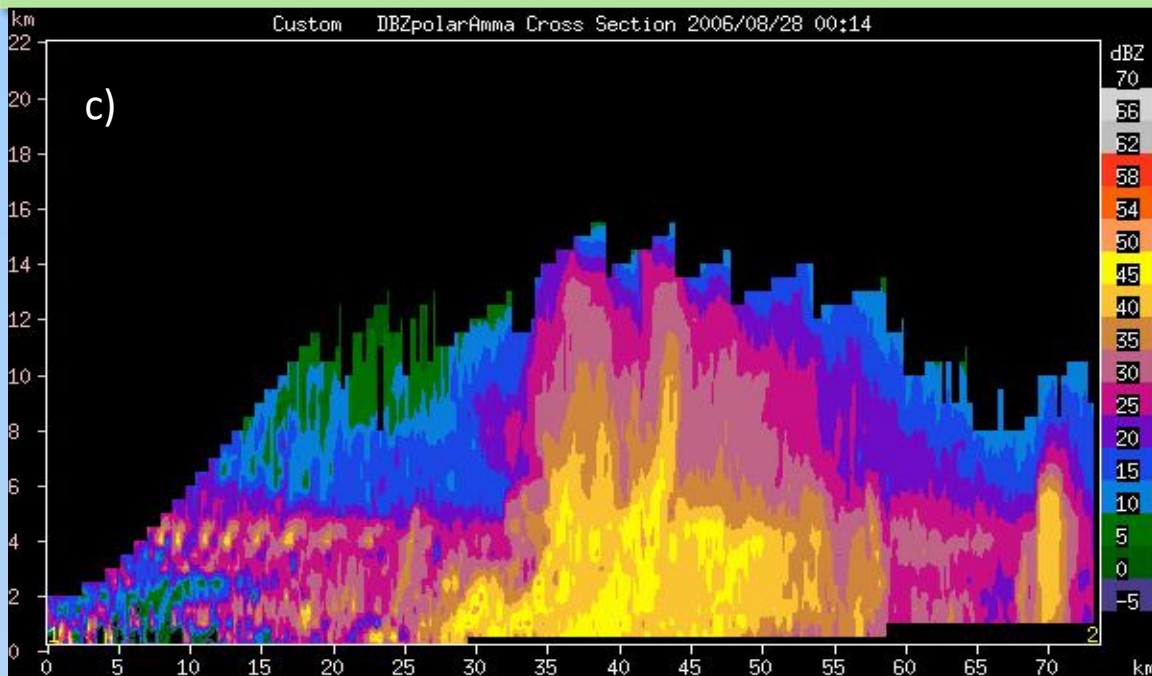
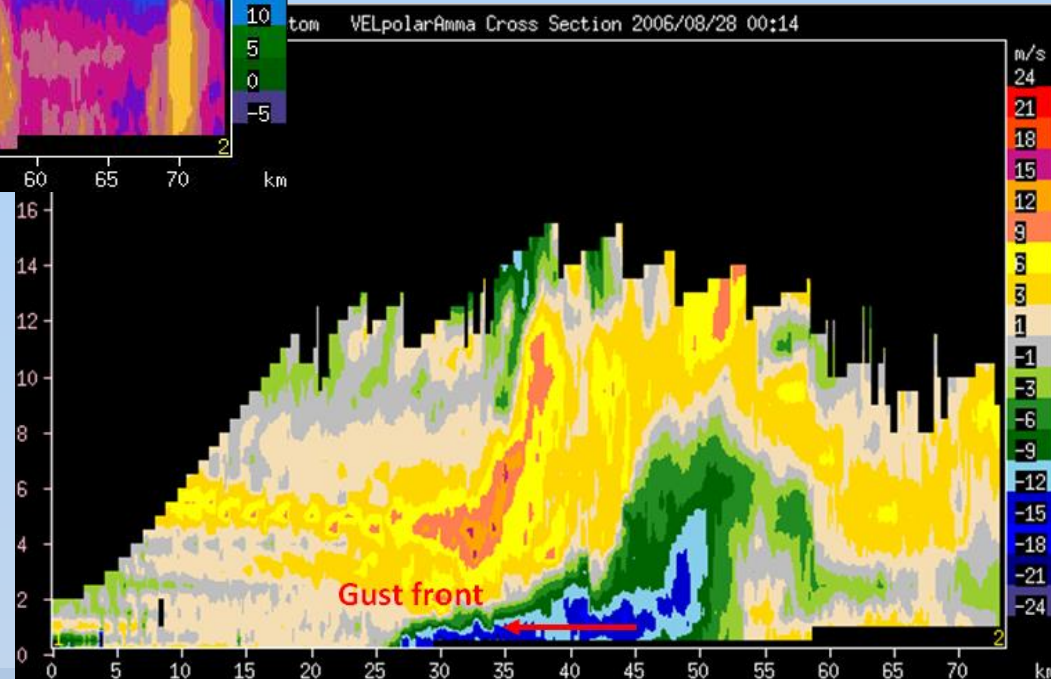


Figure 6.50 cont'd. c) Radar reflectivity (vertical) cross-section (in dBZ). d) Radar radial velocity (vertical) cross-section (in ms⁻¹). Blue and green shades are regions of flow toward the radar, and yellow and red shades are flow away from the radar. Radar position is located to the left of the image. (Source: R. Roberts, 2014)



Chapter 6: Nowcasting – Authors: Rita D. Roberts and James W. Wilson

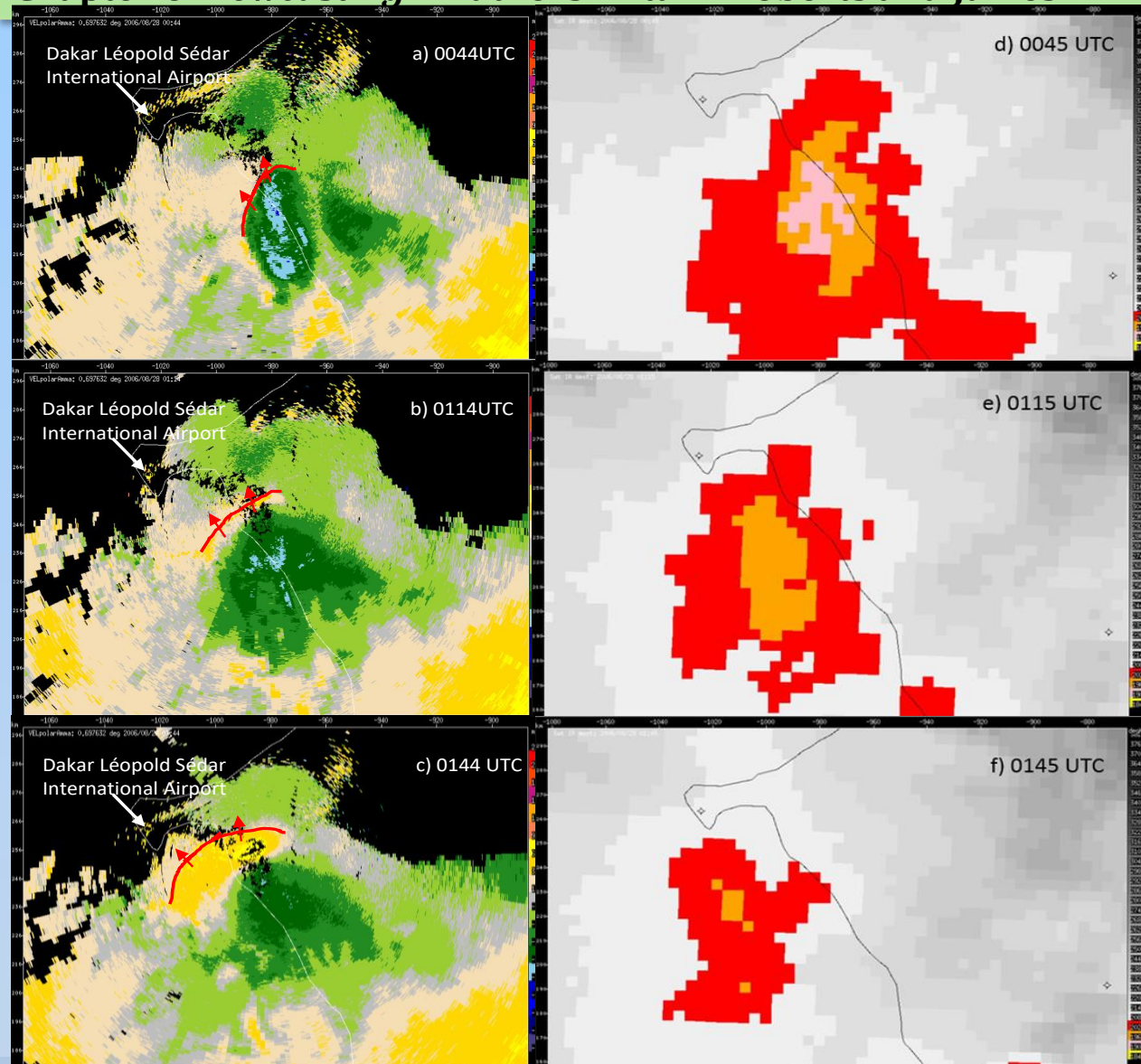


Figure 6.51. a) to c) Gust-front propagation to the northwest over a 90-min period as observed in the NASA NPOL radar radial velocity field. Green and blue shades represent radial winds approaching the radar; yellow and red shades are radial winds moving away from the radar. The radar is located 40 km to the SE of the airport. The red contour and arrows indicate the location of the leading edge of the gust front and its direction of propagation. d) to f) Satellite infrared imagery corresponding to the radar radial velocity data for the same time periods. (Source: R. Roberts, 2014)

Chapter 6: Nowcasting – Authors: Rita D. Roberts and James W. Wilson

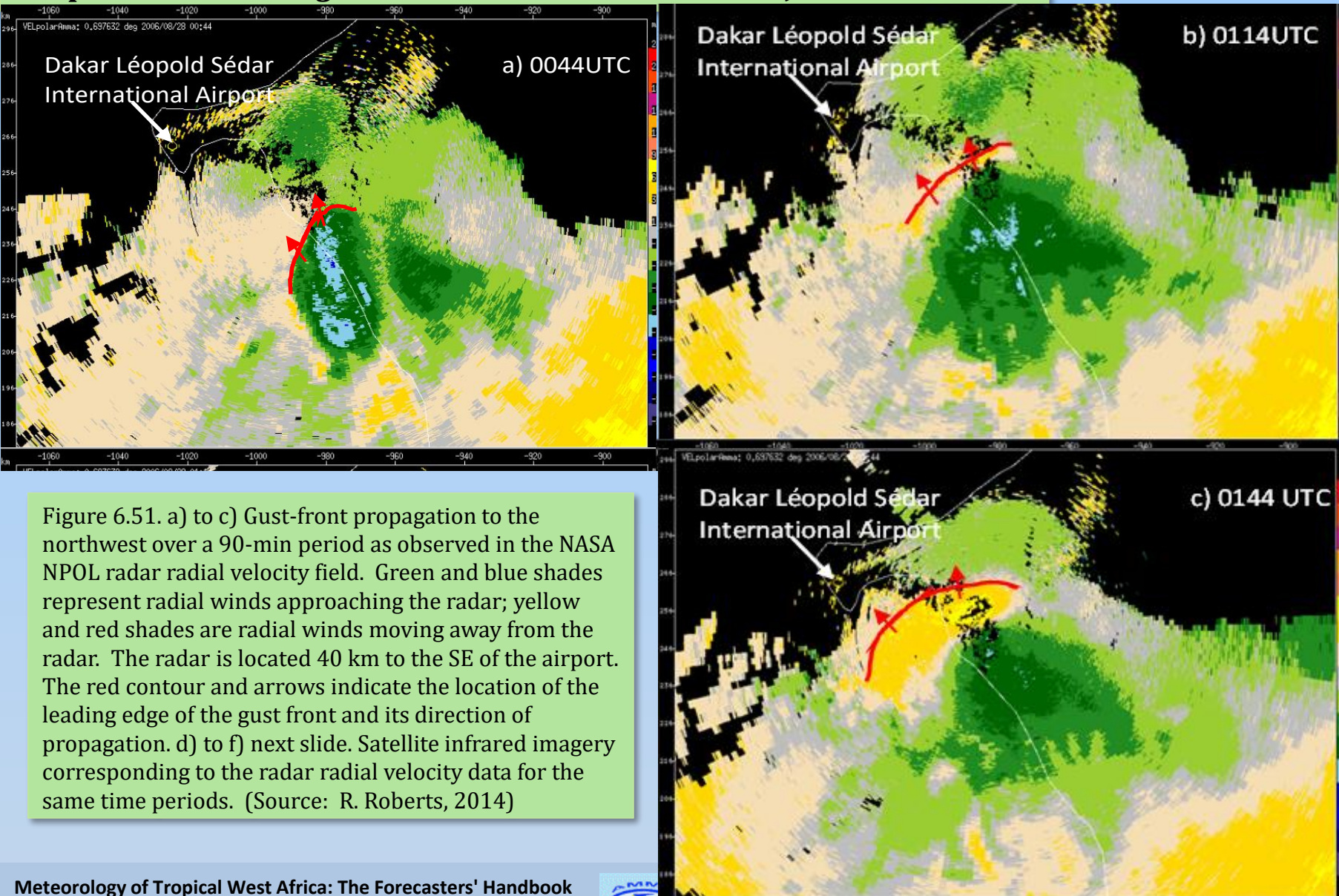


Figure 6.51. a) to c) Gust-front propagation to the northwest over a 90-min period as observed in the NASA NPOL radar radial velocity field. Green and blue shades represent radial winds approaching the radar; yellow and red shades are radial winds moving away from the radar. The radar is located 40 km to the SE of the airport. The red contour and arrows indicate the location of the leading edge of the gust front and its direction of propagation. d) to f) next slide. Satellite infrared imagery corresponding to the radar radial velocity data for the same time periods. (Source: R. Roberts, 2014)

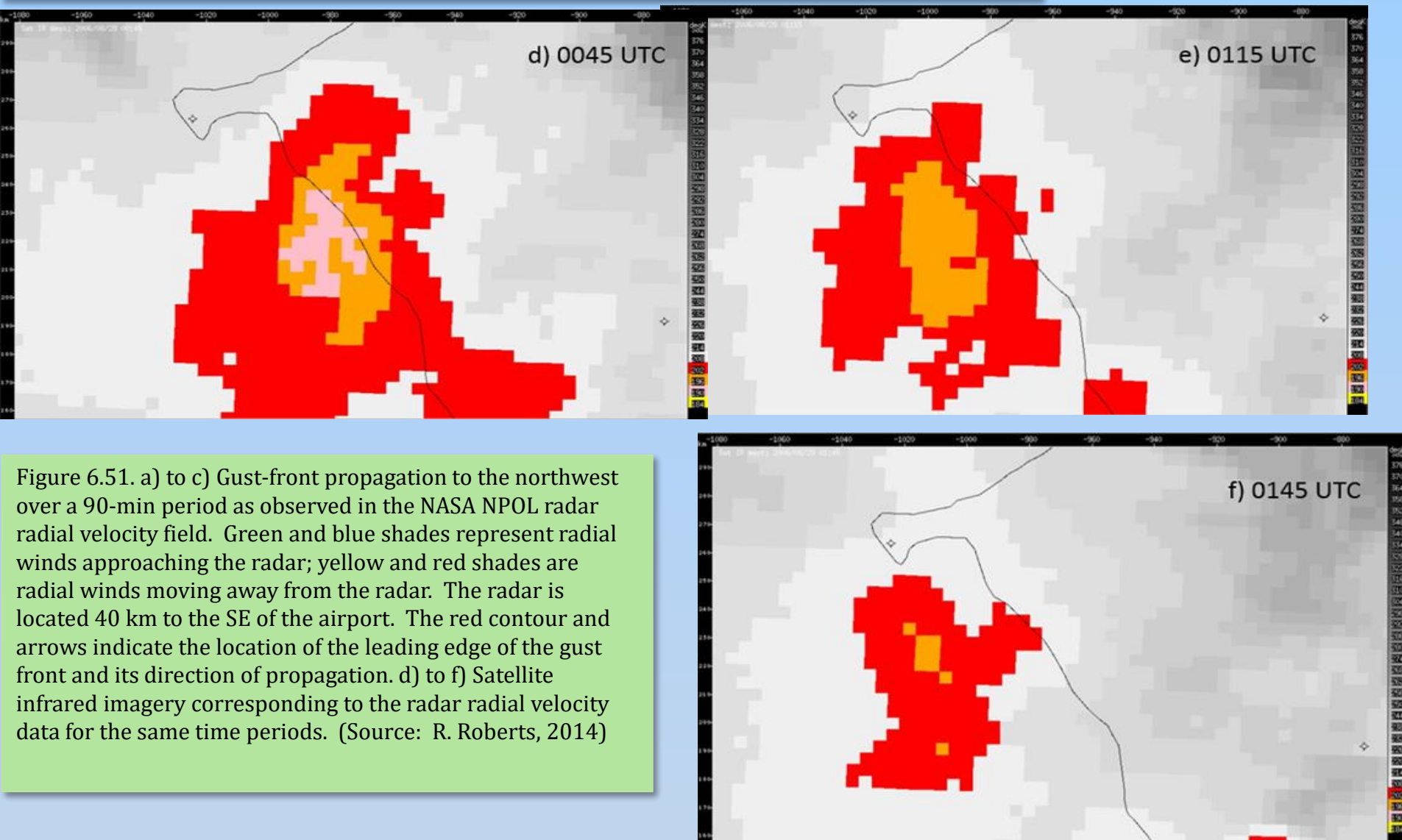


Figure 6.51. a) to c) Gust-front propagation to the northwest over a 90-min period as observed in the NASA NPOL radar radial velocity field. Green and blue shades represent radial winds approaching the radar; yellow and red shades are radial winds moving away from the radar. The radar is located 40 km to the SE of the airport. The red contour and arrows indicate the location of the leading edge of the gust front and its direction of propagation. d) to f) Satellite infrared imagery corresponding to the radar radial velocity data for the same time periods. (Source: R. Roberts, 2014)

Meteorology of Tropical West Africa: The Forecasters' Handbook

Chapter 6: Nowcasting - Authors: Rita D. Roberts and James W. Wilson

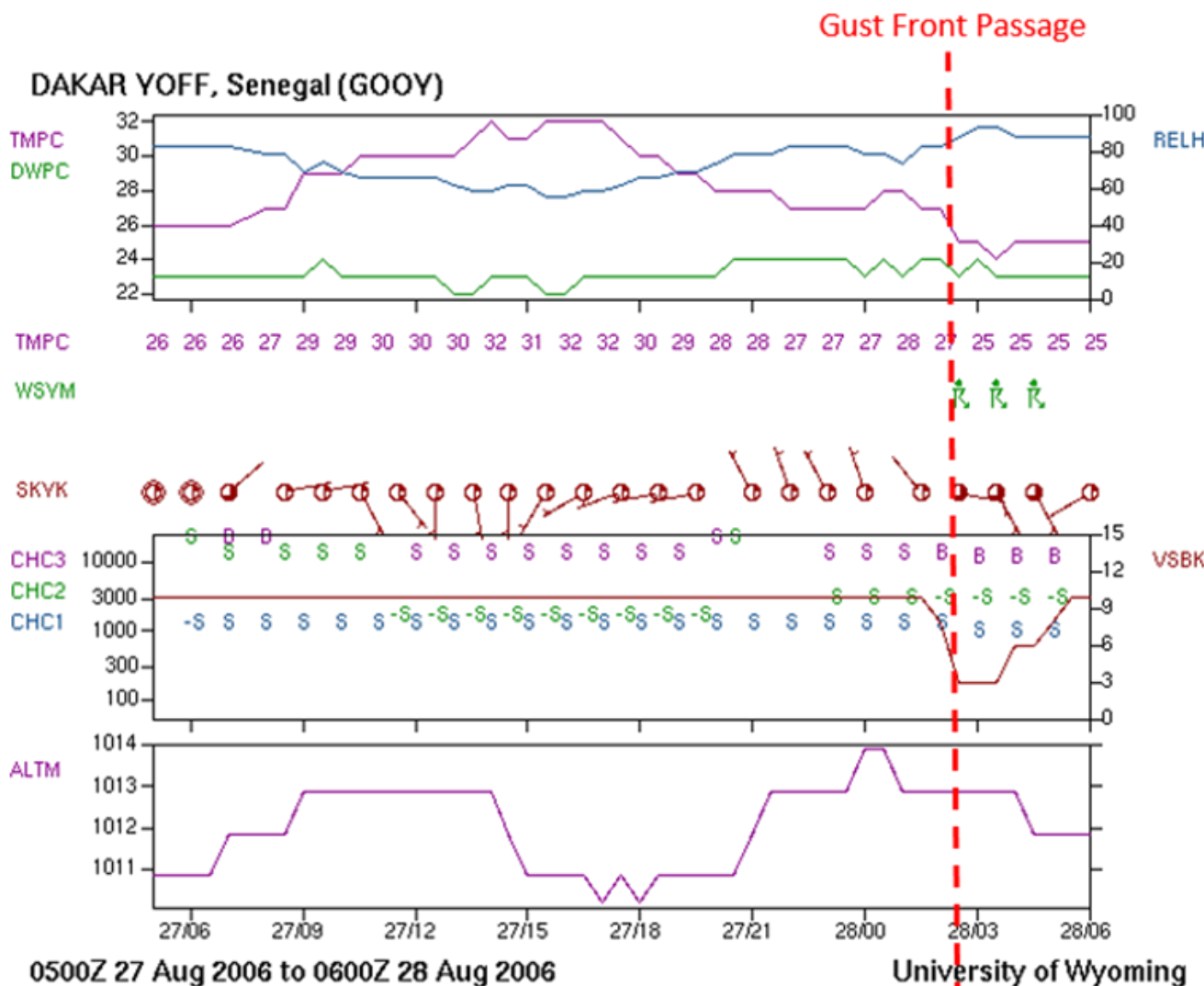


Figure 6.52. Meteogram from surface station at Dakar, Senegal on 27-29 August 2006. Time is shown on the horizontal axis in the form of day/hour. Gust-front passage occurred at approximated 0215 UTC based on meteogram and NPOL radar radial velocity data. In the top panel, temperature ($^{\circ}\text{C}$) is plotted in purple, dewpoint temperature ($^{\circ}\text{C}$) is plotted in green and relative humidity is plotted in blue. In the middle panel, sky conditions are shown in red, the visibility is plotted in brown. The altimeter reading is plotted in purple in the lowest panel. Note that 7.2 mm of rains were recorded at Dakar station. (Source: AMMA Experiment web site, 2014)

Meteorology of Tropical West Africa: The Forecasters' Handbook

Chapter 6: Nowcasting – Authors: Rita D. Roberts and James W. Wilson

ATD Sferic data, starting at 1625 UTC on 28/April/2005. Last updated at 1820

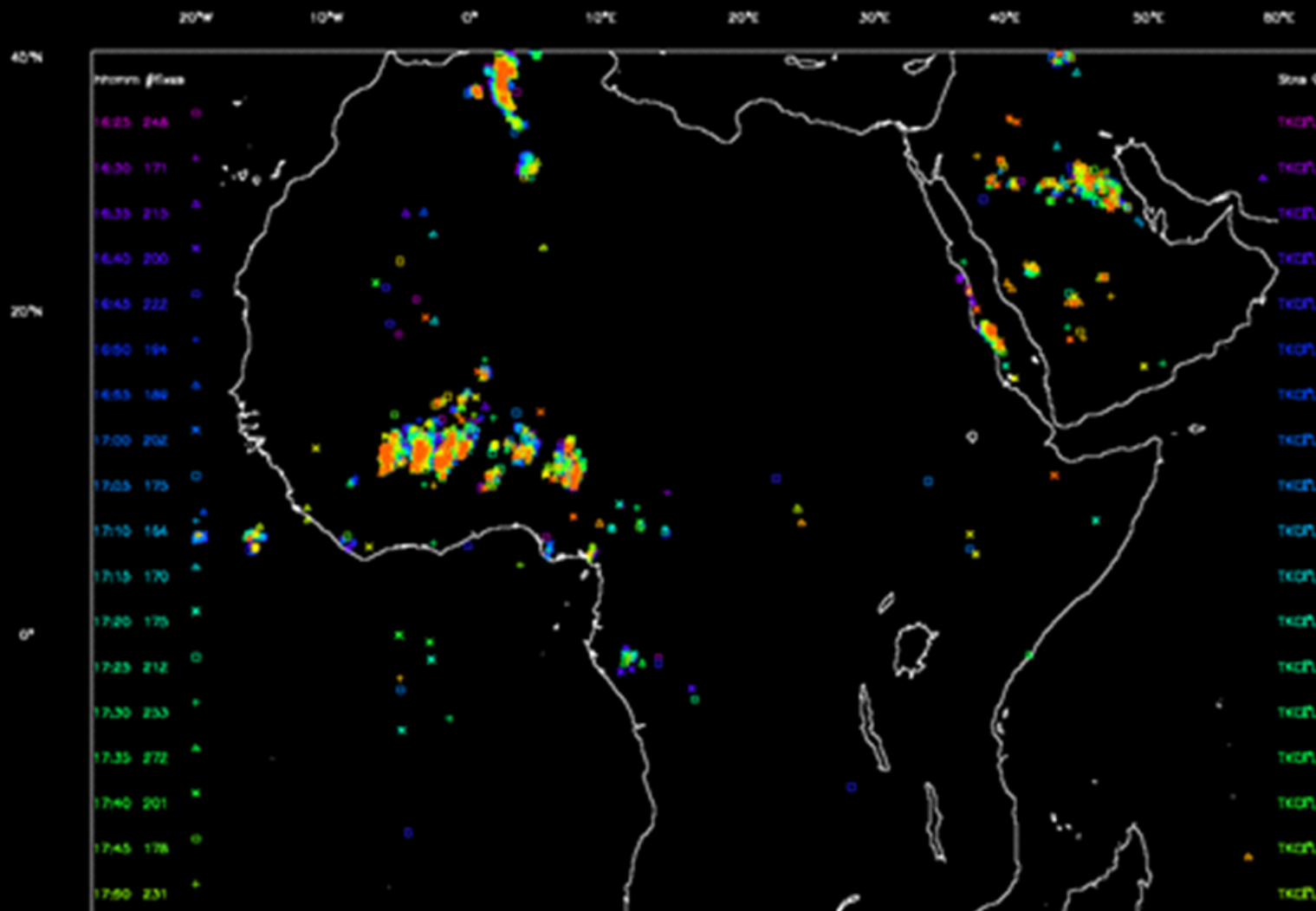


Figure 6.53. ATD sferics returns plotted for a 2-hr period, showing the westward progress of MCS bands over West Africa on 28 April 2005. The most recent sferics (at 1820 UTC) are shown in orange, the oldest (at 1625 UTC) in purple. (Source: J. Galvin, 2014)

Meteorology of Tropical West Africa: The Forecasters' Handbook

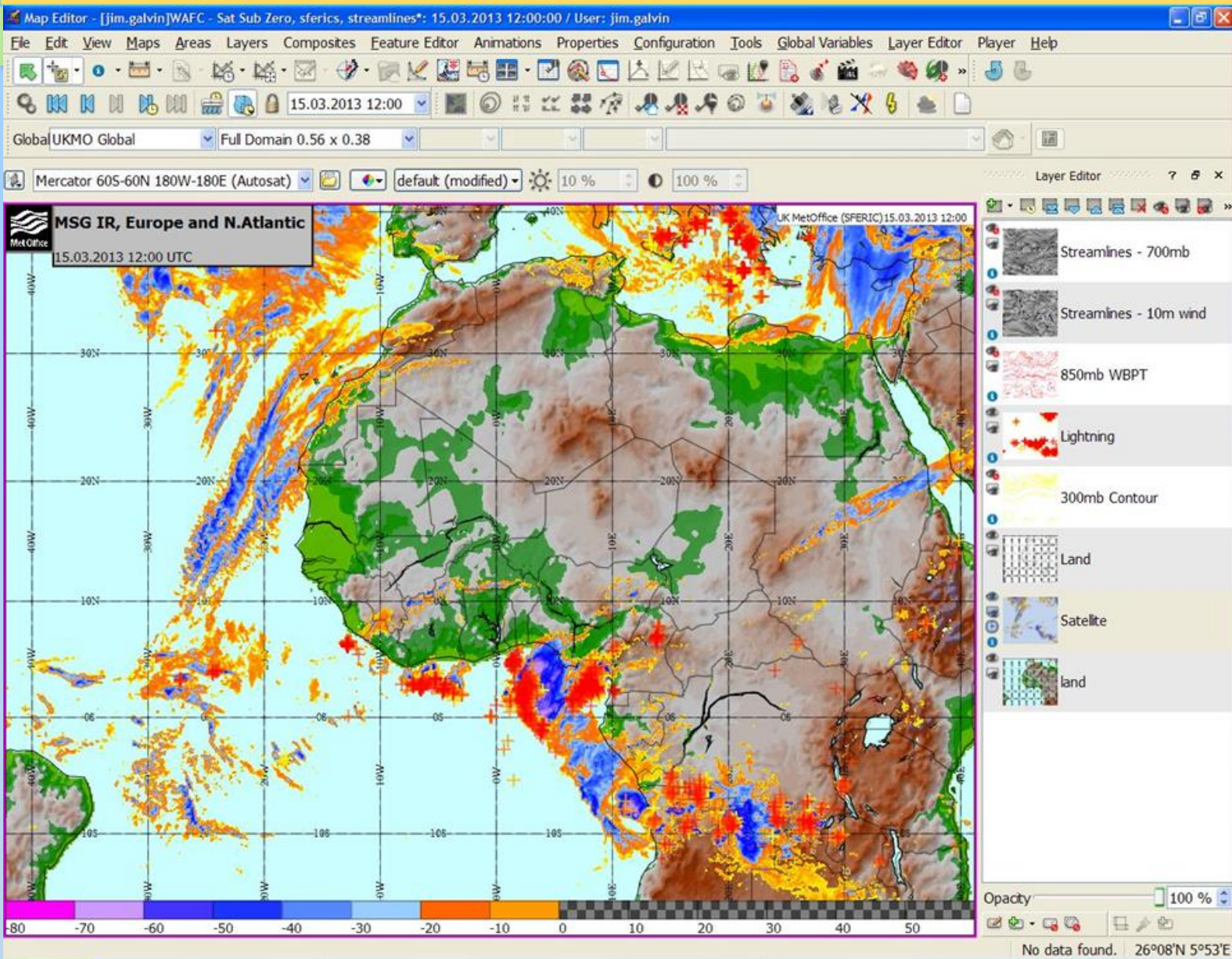


Figure 6.54. (a) Returns from the ATDNET sferics system (crosses) over North Africa overlaid on Infrared cloud imagery (cloud-top temperature colourscale is shown at the bottom of the image) by the Swift/Visual Weather display system. Areas of active deep convection can be seen clearly in the extensive regions of cold cloud-top temperatures (blue shades) and high density of lightning strikes. The sferics plots are coded from red to yellow at 5-min intervals over a total of 60 minutes.